Duct modes in shear flow: properties and applications of the Pridmore-Brown equation

Sjoerd W. Rienstra

CEAA2016 - 4th International Workshop on "Computational Experiment in AeroAcoustics"

Svertlogorsk, Kaliningrad, Russia

21-24 September 2016

Technische Universiteit Eindhoven
University of Technology

Outline

Outline

Where

Turbo engine:

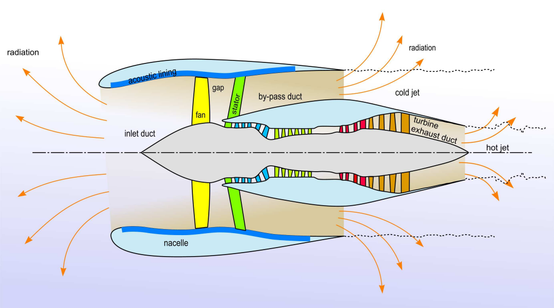

Where

Turbo engine:

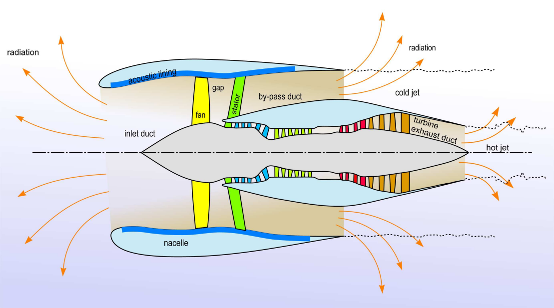

APU:

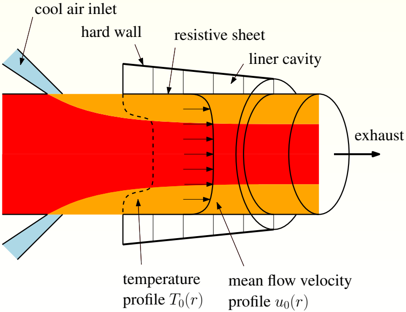

Outline

Origin

- David Clifford Pridmore-Brown developed in the paper

  "Sound propagation in a fluid flowing through an attenuating duct", Journal of Fluid Mechanics, 4, 1958, pp 393 - 406.

  an equation for 2D homentropic modal perturbations in 2D compressible parallel shear flow: the Pridmore-Brown Equation.

- It constitutes an eigenvalue problem for the modes.

- Now we call the radially symmetric 3D version also a Pridmore-Brown Equation, and for the general case (modes along any duct cross section) the Generalised Pridmore-Brown Equation.

Origin

- David Clifford Pridmore-Brown developed in the paper

  "Sound propagation in a fluid flowing through an attenuating duct", Journal of Fluid Mechanics, 4, 1958, pp 393 - 406.

  an equation for 2D homentropic modal perturbations in 2D compressible parallel shear flow: the Pridmore-Brown Equation.

- It constitutes an eigenvalue problem for the modes.

- Now we call the radially symmetric 3D version also a Pridmore-Brown Equation, and for the general case (modes along any duct cross section) the Generalised Pridmore-Brown Equation.

Origin

- David Clifford Pridmore-Brown developed in the paper

  "Sound propagation in a fluid flowing through an attenuating duct", Journal of Fluid Mechanics, 4, 1958, pp 393 - 406.

  an equation for 2D homentropic modal perturbations in 2D compressible parallel shear flow: the Pridmore-Brown Equation.

- It constitutes an eigenvalue problem for the modes.

- Now we call the radially symmetric 3D version also a Pridmore-Brown Equation, and for the general case (modes along any duct cross section) the Generalised Pridmore-Brown Equation.

Linearised Euler equations for perturbations ρ, p, $\boldsymbol{v}$

$$\left(\frac{\partial}{\partial t}+\boldsymbol{V}_0\cdot\nabla\right)\rho+\rho\nabla\cdot\boldsymbol{V}_0+\nabla\cdot(\boldsymbol{v}\rho_0)=0$$
$$\rho_0\left(\frac{\partial}{\partial t}+\boldsymbol{V}_0\cdot\nabla\right)\boldsymbol{v}+\rho_0(\boldsymbol{v}\cdot\nabla)\boldsymbol{V}_0+\rho(\boldsymbol{V}_0\cdot\nabla)\boldsymbol{V}_0=-\nabla p$$
$$\left(\frac{\partial}{\partial t}+\boldsymbol{V}_0\cdot\nabla\right)p-c_0^2\left(\frac{\partial}{\partial t}+\boldsymbol{V}_0\cdot\nabla\right)\rho-c_0^2\boldsymbol{v}\cdot\nabla\rho_0=0$$

For mean parallel shear flow $\boldsymbol{V}_0=U_0(y,z)\boldsymbol{e}_x$, the acoustic field reduces to:

$$D_0^3p+2c_0^2\frac{\partial}{\partial x}(\nabla U_0\cdot\nabla p)-D_0\nabla\cdot(c_0^2\nabla p)=0,\qquad D_0=\frac{\partial}{\partial t}+U_0\frac{\partial}{\partial x}$$

Modes: $p(x,y,z,t)=\mathrm{e}^{\mathrm{i}\omega t-\mathrm{i}kx}P(y,z)$ and $\Omega=\omega-kU_0$, then

$$\frac{\Omega^2}{c_0^2}\nabla\cdot\left(\frac{c_0^2}{\Omega^2}\nabla P\right)+\left(\frac{\Omega^2}{c_0^2}-k^2\right)P=0.$$

Generalised Pridmore-Brown eqn

Cylindrical symmetry: $P(y,z)=P_m(r)\,\mathrm{e}^{-\mathrm{i}m\theta}$

$$\boxed{\frac{\Omega^2}{rc_0^2}\left(\frac{rc_0^2}{\Omega^2}P_m'\right)'+\left(\frac{\Omega^2}{c_0^2}-k^2-\frac{m^2}{r^2}\right)P_m=0}$$

Pridmore-Brown eqn

Linearised Euler equations for perturbations ρ, p, $\boldsymbol{v}$

$$\Big(\frac{\partial}{\partial t} + \boldsymbol{V}_0\cdot\nabla\Big)\rho + \rho\nabla\cdot\boldsymbol{V}_0 + \nabla\cdot\big(\boldsymbol{v}\rho_0\big) = 0$$

$$\rho_0\Big(\frac{\partial}{\partial t} + \boldsymbol{V}_0\cdot\nabla\Big)\boldsymbol{v} + \rho_0\big(\boldsymbol{v}\cdot\nabla\big)\boldsymbol{V}_0 + \rho\big(\boldsymbol{V}_0\cdot\nabla\big)\boldsymbol{V}_0 = -\nabla p$$

$$\Big(\frac{\partial}{\partial t} + \boldsymbol{V}_0\cdot\nabla\Big)p - c_0^2\Big(\frac{\partial}{\partial t} + \boldsymbol{V}_0\cdot\nabla\Big)\rho - c_0^2\boldsymbol{v}\cdot\nabla\rho_0 = 0$$

For mean parallel shear flow $\boldsymbol{V}_0 = U_0(y,z)\boldsymbol{e}_x$, the acoustic field reduces to:

$$D_0^3 p + 2c_0^2\frac{\partial}{\partial x}\big(\nabla U_0\cdot\nabla p\big) - D_0\nabla\cdot\big(c_0^2\nabla p\big) = 0, \qquad D_0=\frac{\partial}{\partial t}+U_0\frac{\partial}{\partial x}$$

Modes: $p(x,y,z,t) = \mathrm{e}^{\mathrm{i}\omega t - \mathrm{i}kx}\, P(y,z)$ and $\Omega = \omega - kU_0$, then

$$\frac{\Omega^2}{c_0^2}\nabla\cdot\Big(\frac{c_0^2}{\Omega^2}\nabla P\Big) + \Big(\frac{\Omega^2}{c_0^2} - k^2\Big)P = 0.$$

Generalised Pridmore-Brown eqn

Cylindrical symmetry: $P(y,z) = P_m(r)\,\mathrm{e}^{-\mathrm{i}m\theta}$

$$\boxed{\frac{\Omega^2}{r c_0^2}\Big(\frac{r c_0^2}{\Omega^2}P_m'\Big)' + \Big(\frac{\Omega^2}{c_0^2} - k^2 - \frac{m^2}{r^2}\Big)P_m = 0}$$

Pridmore-Brown eqn

Linearised Euler equations for perturbations ρ, p, $\boldsymbol{v}$

$$\left(\tfrac{\partial}{\partial t} + \boldsymbol{V}_0 \cdot \nabla\right)\rho + \rho \nabla \cdot \boldsymbol{V}_0 + \nabla \cdot \left(\boldsymbol{v}\rho_0\right) = 0$$

$$\rho_0\left(\tfrac{\partial}{\partial t} + \boldsymbol{V}_0 \cdot \nabla\right)\boldsymbol{v} + \rho_0\left(\boldsymbol{v} \cdot \nabla\right)\boldsymbol{V}_0 + \rho\left(\boldsymbol{V}_0 \cdot \nabla\right)\boldsymbol{V}_0 = -\nabla p$$

$$\left(\tfrac{\partial}{\partial t} + \boldsymbol{V}_0 \cdot \nabla\right)p - c_0^2\left(\tfrac{\partial}{\partial t} + \boldsymbol{V}_0 \cdot \nabla\right)\rho - c_0^2 \boldsymbol{v} \cdot \nabla \rho_0 = 0$$

For mean parallel shear flow $\boldsymbol{V}_0 = U_0(y, z)\boldsymbol{e}_x$, the acoustic field reduces to:

$$D_0^3 p + 2c_0^2 \tfrac{\partial}{\partial x}\left(\nabla U_0 \cdot \nabla p\right) - D_0 \nabla \cdot \left(c_0^2 \nabla p\right) = 0, \qquad D_0 = \tfrac{\partial}{\partial t} + U_0 \tfrac{\partial}{\partial x}$$

Modes: $p(x, y, z, t) = \mathrm{e}^{\mathrm{i}\omega t - \mathrm{i}kx} P(y, z)$ and $\Omega = \omega - kU_0$, then

$$\frac{\Omega^2}{c_0^2}\nabla \cdot \left(\frac{c_0^2}{\Omega^2}\nabla P\right) + \left(\frac{\Omega^2}{c_0^2} - k^2\right)P = 0.$$

Generalised Pridmore-Brown eqn

Cylindrical symmetry: $P(y, z) = P_m(r)\,\mathrm{e}^{-\mathrm{i}m\theta}$

$$\boxed{\frac{\Omega^2}{r c_0^2}\left(\frac{r c_0^2}{\Omega^2}P_m'\right)' + \left(\frac{\Omega^2}{c_0^2} - k^2 - \frac{m^2}{r^2}\right)P_m = 0}$$

Pridmore-Brown eqn

Linearised Euler equations for perturbations ρ, p, $\boldsymbol{v}$

$$\Big(\tfrac{\partial}{\partial t} + \boldsymbol{V}_0\cdot\nabla\Big)\rho + \rho\nabla\cdot\boldsymbol{V}_0 + \nabla\cdot\big(\boldsymbol{v}\rho_0\big) = 0$$
$$\rho_0\Big(\tfrac{\partial}{\partial t} + \boldsymbol{V}_0\cdot\nabla\Big)\boldsymbol{v} + \rho_0\big(\boldsymbol{v}\cdot\nabla\big)\boldsymbol{V}_0 + \rho\big(\boldsymbol{V}_0\cdot\nabla\big)\boldsymbol{V}_0 = -\nabla p$$
$$\Big(\tfrac{\partial}{\partial t} + \boldsymbol{V}_0\cdot\nabla\Big)p - c_0^2\Big(\tfrac{\partial}{\partial t} + \boldsymbol{V}_0\cdot\nabla\Big)\rho - c_0^2\boldsymbol{v}\cdot\nabla\rho_0 = 0$$

For mean parallel shear flow $\boldsymbol{V}_0 = U_0(y,z)\boldsymbol{e}_x$, the acoustic field reduces to:

$$D_0^3 p + 2c_0^2\tfrac{\partial}{\partial x}\big(\nabla U_0\cdot\nabla p\big) - D_0\nabla\cdot\big(c_0^2\nabla p\big) = 0, \qquad D_0 = \tfrac{\partial}{\partial t} + U_0\tfrac{\partial}{\partial x}$$

Modes: $p(x,y,z,t) = \mathrm{e}^{\mathrm{i}\omega t - \mathrm{i}kx}\,P(y,z)$ and $\Omega = \omega - kU_0$, then

$$\frac{\Omega^2}{c_0^2}\nabla\cdot\Big(\frac{c_0^2}{\Omega^2}\nabla P\Big) + \Big(\frac{\Omega^2}{c_0^2} - k^2\Big)P = 0.$$

Generalised Pridmore-Brown eqn

Cylindrical symmetry: $P(y,z) = P_m(r)\,\mathrm{e}^{-\mathrm{i}m\theta}$

$$\boxed{\frac{\Omega^2}{r c_0^2}\Big(\frac{r c_0^2}{\Omega^2}P_m'\Big)' + \Big(\frac{\Omega^2}{c_0^2} - k^2 - \frac{m^2}{r^2}\Big)P_m = 0}$$

Pridmore-Brown eqn

Boundary value problem

Pridmore-Brown equation for $p(x, r, \theta, t) = P(r)\,\mathrm{e}^{\mathrm{i}\omega t - \mathrm{i}m\theta - \mathrm{i}kx}$

$$P'' + \left(\frac{1}{r} + 2\frac{c_0'}{c_0} + 2\frac{ku_0'}{\Omega}\right)P' + \left(\frac{\Omega^2}{c_0^2} - k^2 - \frac{m^2}{r^2}\right)P = 0$$

$+$

Boundary conditions

$$\mathrm{i}\omega Z P' = -\rho_0\Omega^2 P \;\text{ at }\; r = 1, \qquad P \;\text{ is regular at }\; r = 0$$

$=$

Eigenvalue Problem in k

Countable set of modal solutions: $P_{m\mu}(r)\,\mathrm{e}^{-\mathrm{i}k_{m\mu}x}$

- eigenfunctions: $P_{m\mu}(r)$
- eigenvalue (modal axial wavenumber): $k_{m\mu}$

Boundary value problem

Pridmore-Brown equation for $p(x, r, \theta, t) = P(r)\,\mathrm{e}^{\mathrm{i}\omega t - \mathrm{i}m\theta - \mathrm{i}kx}$

$$P'' + \left(\frac{1}{r} + 2\frac{c_0'}{c_0} + 2\frac{ku_0'}{\Omega}\right)P' + \left(\frac{\Omega^2}{c_0^2} - k^2 - \frac{m^2}{r^2}\right)P = 0$$

+

Boundary conditions

$$\mathrm{i}\omega Z P' = -\rho_0\Omega^2 P \text{ at } r = 1, \qquad P \text{ is regular at } r = 0$$

=

Eigenvalue Problem in k

Countable set of modal solutions: $P_{m\mu}(r)\,\mathrm{e}^{-\mathrm{i}k_{m\mu}x}$

- eigenfunctions: $P_{m\mu}(r)$
- eigenvalue (modal axial wavenumber): $k_{m\mu}$

Boundary value problem

Pridmore-Brown equation for $p(x, r, \theta, t) = P(r)\, \mathrm{e}^{\mathrm{i}\omega t - \mathrm{i}m\theta - \mathrm{i}kx}$

$$P'' + \left(\frac{1}{r} + 2\frac{c_0'}{c_0} + 2\frac{ku_0'}{\Omega}\right) P' + \left(\frac{\Omega^2}{c_0^2} - k^2 - \frac{m^2}{r^2}\right) P = 0$$

+

Boundary conditions

$\mathrm{i}\omega Z P' = -\rho_0 \Omega^2 P$ at $r = 1$, $\qquad P$ is regular at $r = 0$

=

Eigenvalue Problem in k

Countable set of modal solutions: $P_{m\mu}(r)\, \mathrm{e}^{-\mathrm{i}k_{m\mu}x}$

- eigenfunctions: $P_{m\mu}(r)$
- eigenvalue (modal axial wavenumber): $k_{m\mu}$

Outline

How do we find “all” modes:

- Start with a simple configuration
- Parameter continuation in
  - Impedance Z
  - Mean flow profile u_0, c_0

How do we find "all" modes:

- Start with a simple configuration
- Parameter continuation in
  - Impedance Z
  - Mean flow profile u_0, c_0

How do we find “all” modes:

- Start with a simple configuration
- Parameter continuation in
  - Impedance Z
  - Mean flow profile u_0, c_0

How do we find “all” modes:

- Start with a simple configuration
- Parameter continuation in
  - Impedance Z
  - Mean flow profile u_0, c_0

How do we find “all” modes:

- Start with a simple configuration
- Parameter continuation in
  - Impedance Z
  - Mean flow profile u_0, c_0

Example of path-following

In duct, eigenvalues $k_{m\mu}$ follows from impedance boundary condition.

Example* of path-following in $Z : \infty \to \infty$

Note the surface waves: instability

---

* *with* $\mathrm{e}^{-\mathrm{i}\omega t}$*-convention…*

Example of path-following

In duct, eigenvalues $k_{m\mu}$ follows from impedance boundary condition.

Example* of path-following in $Z : \infty \rightarrow \infty$

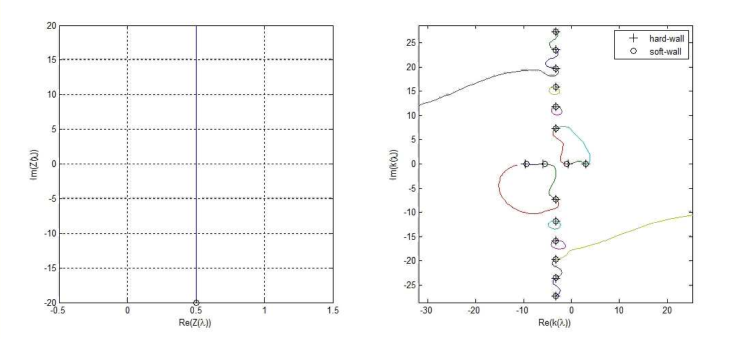

Z-plane $\qquad$ k-plane

Note the surface waves: instability

---

* *with* $\mathrm{e}^{-\mathrm{i}\omega t}$*-convention…*

Example of path-following

In duct, eigenvalues $k_{m\mu}$ follows from impedance boundary condition.

Example* of path-following in $Z : \infty \to \infty$

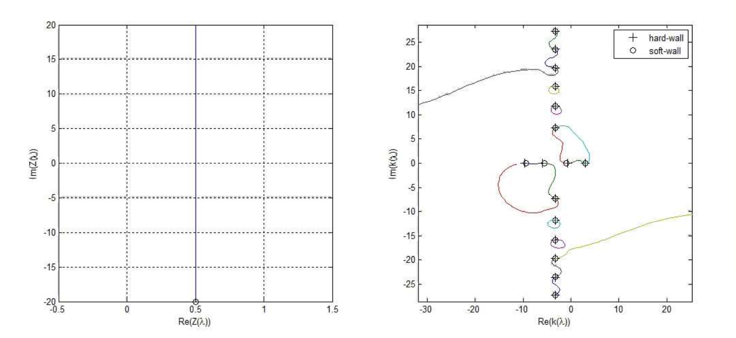

Z-plane $\qquad$ k-plane

Note the surface waves: instability

---

* *with* $\mathrm{e}^{-\mathrm{i}\omega t}$*-convention. . .*

Numerical results: eigenfunctions & eigenvalues

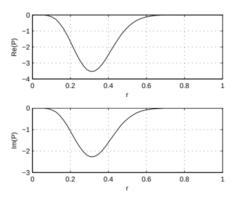

(a) $\mu = 1$

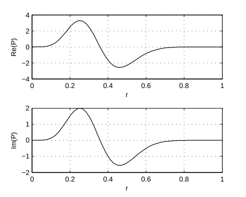

(b) $\mu = 2$

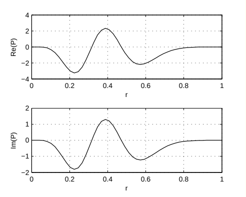

(c) $\mu = 3$

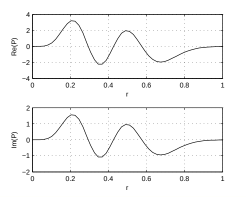

(d) $\mu = 4$

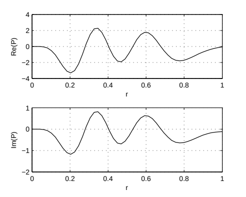

(e) $\mu = 5$

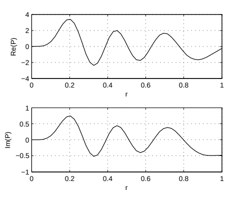

(f) $\mu = 6$

Eigenfunctions for upstream-running modes, $\omega = 25$, $m = 5$, $Z = 2 - \mathrm{i}$, $u_0 = \frac{2}{3}(1 - \frac{1}{2}r^2)$, uniform temperature.
Note: modes $\mu = $ 1-4 confined to core. "Shooting" not possible.

Numerical results: eigenfunctions & eigenvalues

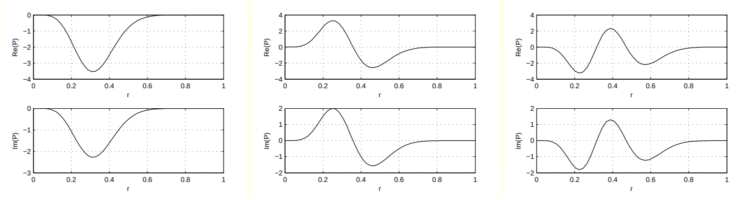

(a) $\mu = 1$ (b) $\mu = 2$ (c) $\mu = 3$

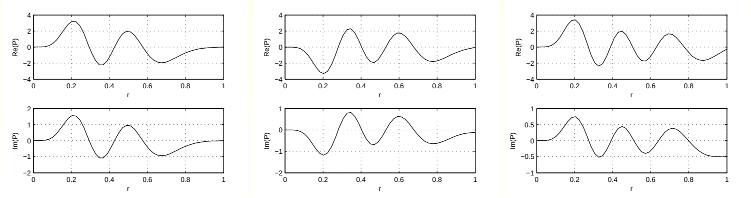

(d) $\mu = 4$ (e) $\mu = 5$ (f) $\mu = 6$

Eigenfunctions for upstream-running modes, $\omega = 25$, $m = 5$, $Z = 2 - \mathrm{i}$, $u_0 = \frac{2}{3}(1 - \frac{1}{2}r^2)$, uniform temperature.

Note: modes $\mu = 1$-4 confined to core. "Shooting" not possible.

Numerical results: further tests

Test case borrowed from quantum-mechanical potential well problem:

- Pridmore-Brown equation:

$$P'' + \beta(r,k)P' + \gamma(r,k)P = 0$$

- *Quantisation condition* based on WKB-type (high-k) approximation

$$\int_{r_1}^{r_2} \sqrt{\gamma(r,k)}\,\mathrm{d}r = (n - \tfrac{1}{2})\pi, \quad n = 1, 2, \ldots$$

μ	k_{QC}	$k_{\mathrm{numerical}}$
1	-60.470038	-60.4392
2	-55.761464	-55.7281
3	-51.134207	-51.0980 - 0.0000i
4	-46.605323	-46.5659 - 0.0003i
5	-42.195790	-42.1422 - 0.0212i
6	-37.931052	-37.5622 - 0.3254i

k's for upstream-running modes.

- Excellent agreement

Numerical results: further tests

Test case borrowed from quantum-mechanical potential well problem:

- Pridmore-Brown equation:

$$P'' + \beta(r,k)P' + \gamma(r,k)P = 0$$

- *Quantisation condition* based on WKB-type (high-k) approximation

$$\int_{r_1}^{r_2} \sqrt{\gamma(r,k)}\,\mathrm{d}r = (n - \tfrac{1}{2})\pi, \quad n = 1, 2, \ldots$$

μ	k_{QC}	$k_{\mathrm{numerical}}$
1	-60.470038	-60.4392
2	-55.761464	-55.7281
3	-51.134207	-51.0980 - 0.0000i
4	-46.605323	-46.5659 - 0.0003i
5	-42.195790	-42.1422 - 0.0212i
6	-37.931052	-37.5622 - 0.3254i

k's for upstream-running modes.

- Excellent agreement

Numerical results: further tests

Test case borrowed from quantum-mechanical potential well problem:

- Pridmore-Brown equation:

$$P'' + \beta(r,k)P' + \gamma(r,k)P = 0$$

- *Quantisation condition* based on WKB-type (high-k) approximation

$$\int_{r_1}^{r_2} \sqrt{\gamma(r,k)}\,\mathrm{d}r = (n - \tfrac{1}{2})\pi, \quad n = 1, 2, \ldots$$

μ	k_{QC}	$k_{\mathrm{numerical}}$
1	-60.470038	-60.4392
2	-55.761464	-55.7281
3	-51.134207	-51.0980 - 0.0000i
4	-46.605323	-46.5659 - 0.0003i
5	-42.195790	-42.1422 - 0.0212i
6	-37.931052	-37.5622 - 0.3254i

k's for upstream-running modes.

- Excellent agreement

Evidently, we obtain mode patterns like

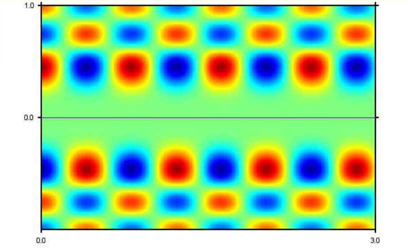

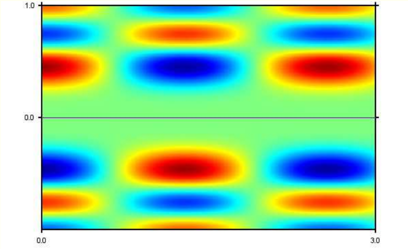

Outline

A canonical model for sound in sheared flow

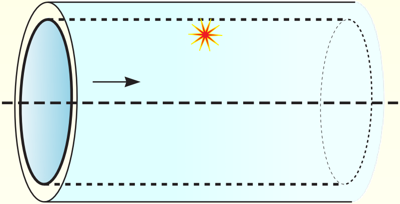

- Linearised Euler flow.
- Uniform velocity profile with finite boundary layers (shear).
- Wall lined by impedance.
- Point mass source.

Time-harmonic pressure field in Fourier representation

$$p(x, r, \theta, t) = \mathrm{e}^{\mathrm{i}\omega t} \sum_{m=-\infty}^{\infty} \mathrm{e}^{-\mathrm{i}m\theta} \int_{-\infty}^{\infty} \tilde{p}_m(r, k)\, \mathrm{e}^{-\mathrm{i}kx}\, \mathrm{d}k.$$

Pridmore-Brown equation for $\tilde{p}$ and point mass source at $(x, \theta, r) = (0, 0, r_0)$

$$\tilde{p}'' + \Big(\frac{1}{r} + \frac{2kU'}{\omega - kU} - \frac{\rho_0'}{\rho_0}\Big)\tilde{p}' + \Big((\omega - kU)^2 - k^2 - \frac{m^2}{r^2}\Big)\tilde{p} = \frac{\omega - U(r_0)k}{2\pi \mathrm{i} r_0}\delta(r - r_0)$$

$U(1) = 0$, $\tilde{p}$ regular in $r = 0$, impedance condition at wall. Singularity.

A canonical model for sound in sheared flow

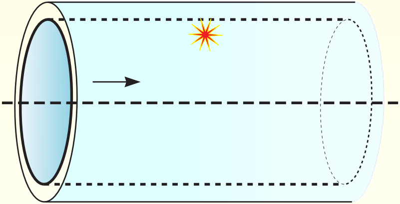

- Linearised Euler flow.
- Uniform velocity profile with finite boundary layers (shear).
- Wall lined by impedance.
- Point mass source.

Time-harmonic pressure field in Fourier representation

$$p(x, r, \theta, t) = \mathrm{e}^{\mathrm{i}\omega t} \sum_{m=-\infty}^{\infty} \mathrm{e}^{-\mathrm{i}m\theta} \int_{-\infty}^{\infty} \tilde{p}_m(r, k)\, \mathrm{e}^{-\mathrm{i}kx}\, \mathrm{d}k.$$

Pridmore-Brown equation for $\tilde{p}$ and point mass source at $(x, \theta, r) = (0, 0, r_0)$

$$\tilde{p}'' + \Big(\frac{1}{r} + \frac{2kU'}{\omega - kU} - \frac{\rho_0'}{\rho_0}\Big)\tilde{p}' + \Big((\omega - kU)^2 - k^2 - \frac{m^2}{r^2}\Big)\tilde{p} = \frac{\omega - U(r_0)k}{2\pi \mathrm{i} r_0}\delta(r - r_0)$$

$U(1) = 0$, $\tilde{p}$ regular in $r = 0$, impedance condition at wall. Singularity.

A canonical model for sound in sheared flow

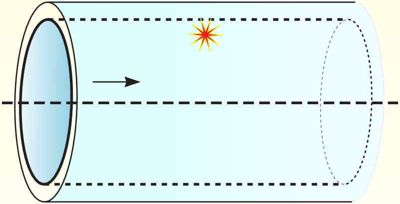

- Linearised Euler flow.
- Uniform velocity profile with finite boundary layers (shear).
- Wall lined by impedance.
- Point mass source.

Time-harmonic pressure field in Fourier representation

$$p(x, r, \theta, t) = \mathrm{e}^{\mathrm{i}\omega t} \sum_{m=-\infty}^{\infty} \mathrm{e}^{-\mathrm{i}m\theta} \int_{-\infty}^{\infty} \tilde{p}_m(r, k)\, \mathrm{e}^{-\mathrm{i}kx}\, \mathrm{d}k.$$

Pridmore-Brown equation for $\tilde{p}$ and point mass source at $(x, \theta, r) = (0, 0, r_0)$

$$\tilde{p}'' + \left(\frac{1}{r} + \frac{2kU'}{\omega - kU} - \frac{\rho_0'}{\rho_0}\right)\tilde{p}' + \left((\omega - kU)^2 - k^2 - \frac{m^2}{r^2}\right)\tilde{p} = \frac{\omega - U(r_0)k}{2\pi \mathrm{i} r_0}\delta(r - r_0)$$

$U(1) = 0$, $\tilde{p}$ regular in $r = 0$, impedance condition at wall. Singularity.

A canonical model for sound in sheared flow

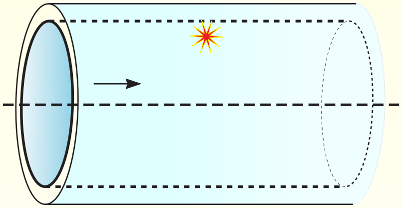

- Linearised Euler flow.
- Uniform velocity profile with finite boundary layers (shear).
- Wall lined by impedance.
- Point mass source.

Time-harmonic pressure field in Fourier representation

$$p(x,r,\theta,t) = \mathrm{e}^{\mathrm{i}\omega t}\sum_{m=-\infty}^{\infty}\mathrm{e}^{-\mathrm{i}m\theta}\int_{-\infty}^{\infty}\tilde{p}_m(r,k)\,\mathrm{e}^{-\mathrm{i}kx}\,\mathrm{d}k.$$

Pridmore-Brown equation for $\tilde{p}$ and point mass source at $(x,\theta,r)=(0,0,r_0)$

$$\tilde{p}''+\Big(\frac{1}{r}+\frac{2kU'}{\omega-kU}-\frac{\rho_0'}{\rho_0}\Big)\tilde{p}'+\Big((\omega-kU)^2-k^2-\frac{m^2}{r^2}\Big)\tilde{p} = \frac{\omega-U(r_0)k}{2\pi\mathrm{i}r_0}\delta(r-r_0)$$

$U(1)=0$, $\tilde{p}$ regular in $r=0$, impedance condition at wall. Singularity.

A canonical model for sound in sheared flow

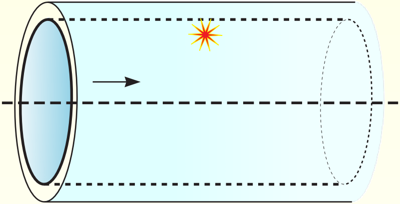

- Linearised Euler flow.
- Uniform velocity profile with finite boundary layers (shear).
- Wall lined by impedance.
- Point mass source.

Time-harmonic pressure field in Fourier representation

$$p(x,r,\theta,t) = \mathrm{e}^{\mathrm{i}\omega t} \sum_{m=-\infty}^{\infty} \mathrm{e}^{-\mathrm{i}m\theta} \int_{-\infty}^{\infty} \tilde{p}_m(r,k)\, \mathrm{e}^{-\mathrm{i}kx}\, \mathrm{d}k.$$

Pridmore-Brown equation for $\tilde{p}$ and point mass source at $(x,\theta,r) = (0,0,r_0)$

$$\tilde{p}'' + \left(\frac{1}{r} + \frac{2kU'}{\omega - kU} - \frac{\rho_0'}{\rho_0}\right)\tilde{p}' + \left((\omega - kU)^2 - k^2 - \frac{m^2}{r^2}\right)\tilde{p} = \frac{\omega - U(r_0)k}{2\pi\mathrm{i}r_0}\delta(r - r_0)$$

$U(1) = 0$, $\tilde{p}$ regular in $r = 0$, impedance condition at wall. Singularity.

Typical properties

- Acoustic modes
- Hydrodynamic instabilities and other surface waves
- Critical layers $\omega - kU = 0$: modal phase speed = mean flow velocity

*singularity $\rightarrow$ branch point of complex logarithm in k-plane

Typical properties

- Acoustic modes
- Hydrodynamic instabilities and other surface waves
- Critical layers* $\omega - kU = 0$: modal phase speed = mean flow velocity

*singularity $\rightarrow$ branch point of complex logarithm in k-plane

Typical properties

- Acoustic modes
- Hydrodynamic instabilities and other surface waves
- Critical layers* $\omega - kU = 0$: modal phase speed = mean flow velocity

*singularity $\rightarrow$ branch point of complex logarithm in k-plane

Typical properties

- Acoustic modes
- Hydrodynamic instabilities and other surface waves
- Critical layers* $\omega - kU = 0$: modal phase speed = mean flow velocity

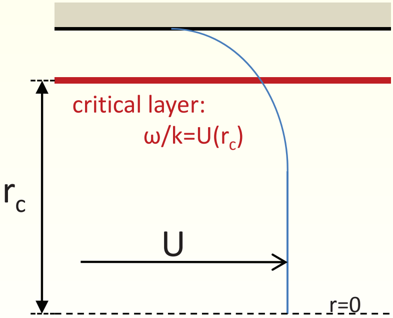

*singularity $\rightarrow$ branch point of complex logarithm in k-plane

Typical properties

- Acoustic modes
- Hydrodynamic instabilities and other surface waves
- Critical layers* $\omega - kU = 0$: modal phase speed = mean flow velocity

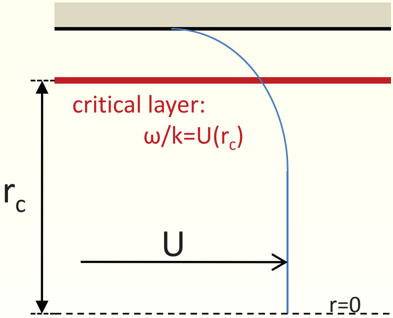

*singularity $\rightarrow$ branch point of complex logarithm in k-plane

Overview of the k-plane (m fixed)

- acoustic poles $k_{m\mu}$
- branch cut
- k_0 (source in BL)
- 2 additional poles
  - k_+ (instability);
  - k_- (associated to branch cut)
- causal integration contour
- close $\curvearrowleft$ for $x < 0$ (modes)
- close $\circlearrowleft$ for $x > 0$ (modes + bc)

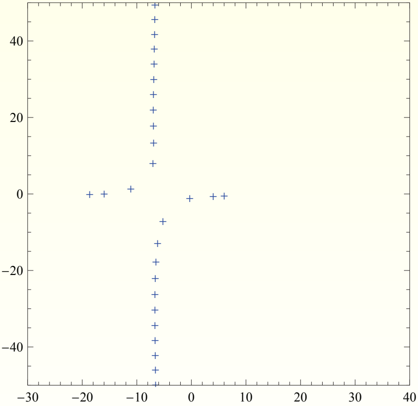

Overview of the k-plane (m fixed)

- acoustic poles $k_{m\mu}$
- branch cut
- k_0 (source in BL)
- 2 additional poles
  - k_+ (instability);
  - k_- (associated to branch cut)
- causal integration contour
- close $\curvearrowleft$ for $x < 0$ (modes)
- close $\curvearrowright$ for $x > 0$ (modes + bc)

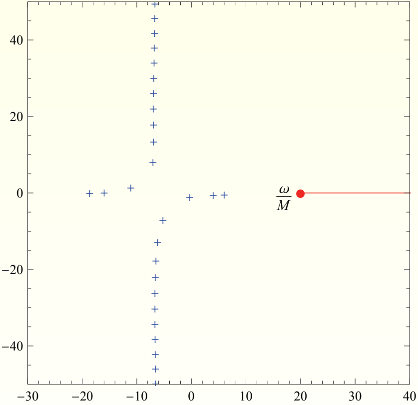

Overview of the k-plane (m fixed)

- acoustic poles $k_{m\mu}$
- branch cut
- k_0 (source in BL)
- 2 additional poles
  - k_+ (instability);
  - k_- (associated to branch cut)
- causal integration contour
- close $\curvearrowleft$ for $x < 0$ (modes)
- close $\curvearrowright$ for $x > 0$ (modes + bc)

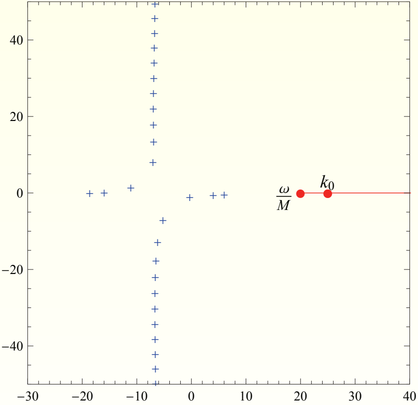

Overview of the k-plane (m fixed)

- acoustic poles $k_{m\mu}$
- branch cut
- k_0 (source in BL)
- 2 additional poles
  - k_+ (instability);
  - k_- (associated to branch cut)
- causal integration contour
- close $\curvearrowleft$ for $x < 0$ (modes)
- close $\curvearrowright$ for $x > 0$ (modes + bc)

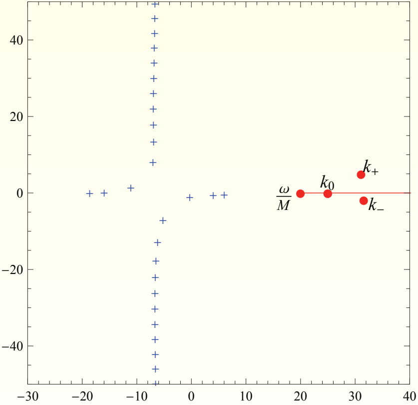

Overview of the k-plane (m fixed)

- acoustic poles $k_{m\mu}$
- branch cut
- k_0 (source in BL)
- 2 additional poles
  - k_+ (instability);
  - k_- (associated to branch cut)
- causal integration contour
- close ↶ for $x < 0$ (modes)
- close ↷ for $x > 0$ (modes + bc)

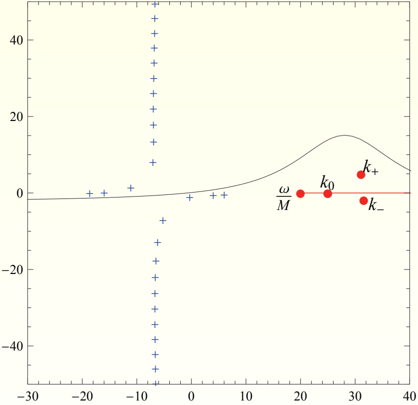

Overview of the k-plane (m fixed)

- acoustic poles $k_{m\mu}$
- branch cut
- k_0 (source in BL)
- 2 additional poles
  - k_+ (instability);
  - k_- (associated to branch cut)
- causal integration contour
- close $\curvearrowleft$ for $x < 0$ (modes)
- close $\circlearrowright$ for $x > 0$ (modes + bc)

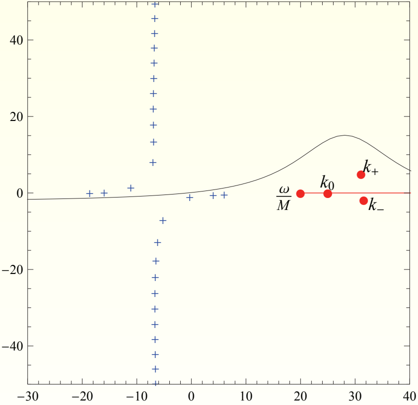

Overview of the k-plane (m fixed)

- acoustic poles $k_{m\mu}$
- branch cut
- k_0 (source in BL)
- 2 additional poles
  - k_+ (instability);
  - k_- (associated to branch cut)
- causal integration contour
- close $\curvearrowleft$ for $x < 0$ (modes)
- close $\circlearrowleft$ for $x > 0$ (modes + bc)

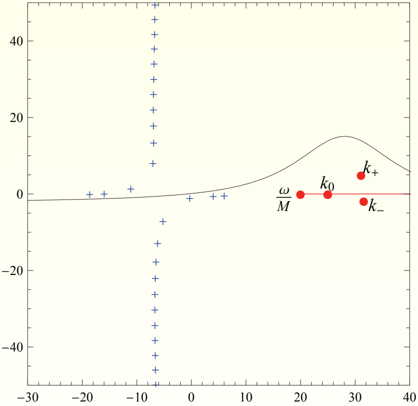

Examples. $M = 0.5$, $\omega = 10$, $m = 0$, $Z = 2 - \mathrm{i}$

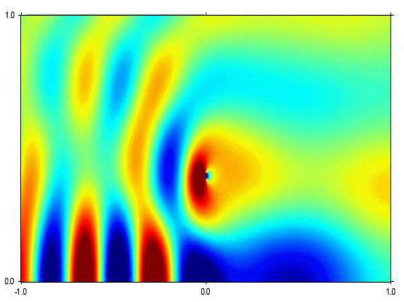

$h = 0.001$, $r_0 = 0.4$, $Z = 2 + \mathrm{i}$

Examples. $M = 0.5$, $\omega = 10$, $m = 0$, $Z = 2 - \mathrm{i}$

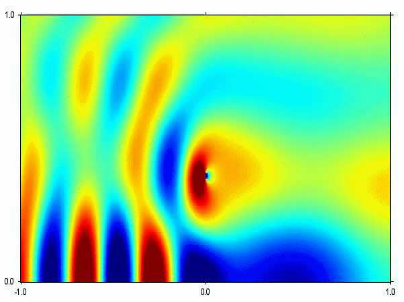

$h = 0.001$, $r_0 = 0.4$, $Z = 2 + \mathrm{i}$

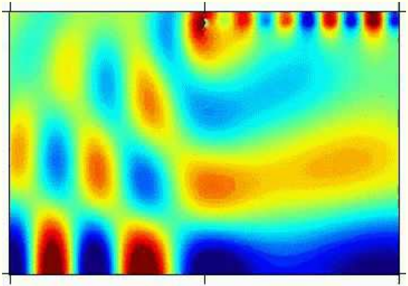

$h = 0.05$, $r_0 = 0.96$ (vortices from source)

Examples. $M = 0.5$, $\omega = 10$, $m = 0$, $Z = 2 - \mathrm{i}$

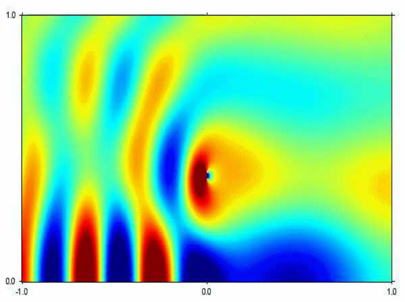

$h = 0.001$, $r_0 = 0.4$, $Z = 2 + \mathrm{i}$

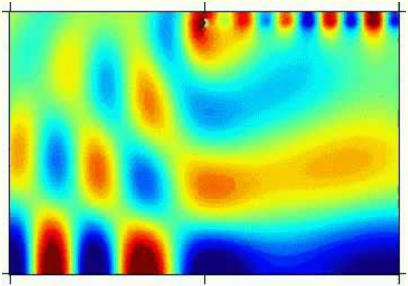

$h = 0.05$, $r_0 = 0.96$ (vortices from source)

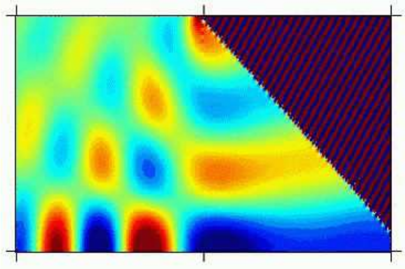

$h = 0.001$, $r_0 = 0.992$ (instability from source)

Examples. $M = 0.5$, $\omega = 10$, $m = 0$, $Z = 2 - \mathrm{i}$

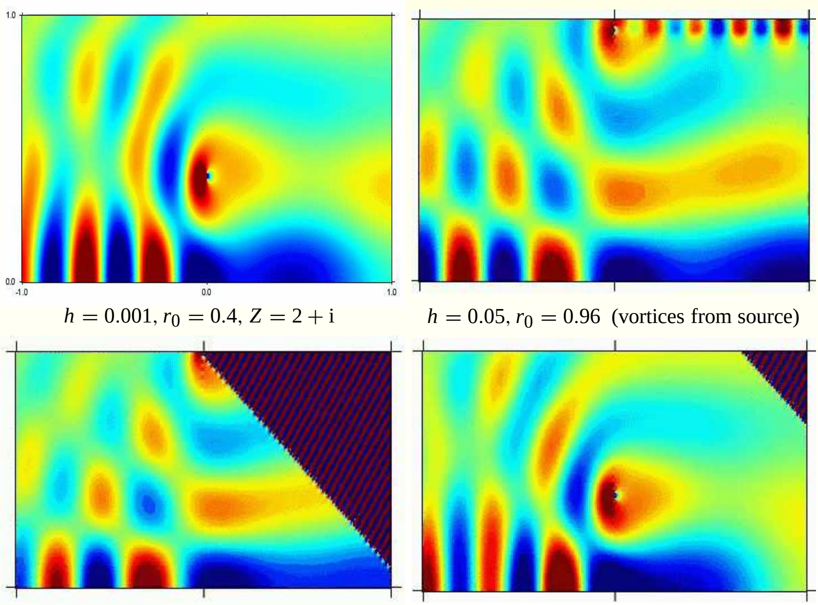

$h = 0.001$, $r_0 = 0.4$, $Z = 2 + \mathrm{i}$ $h = 0.05$, $r_0 = 0.96$ (vortices from source)

$h = 0.001$, $r_0 = 0.992$ (instability from source) $h = 0.001$, $r_0 = 0.4$ (instability from outside)

Interim conclusions

- The contribution from the branch cut and its associated pole is very minor unless all acoustic modes are cut-off. So it makes sense to use the acoustic modes as a "complete" basis to construct a general solution.
- Trailing vortices in boundary layer.
- The relevance of the spatial instability.
- The (related) question of the limit of $h \to 0$ (the Ingard-Myers limit): the boundary condition with $U_{\text{wall}} = 0$ changes to an equivalent boundary condition for U_{wall} finite.

$$\mathrm{i}\omega Z\tilde{v} = \left(\mathrm{i}\omega + U_{\text{wall}}\frac{\partial}{\partial x}\right)\tilde{p}$$

How physical is this?

Interim conclusions

- The contribution from the branch cut and its associated pole is very minor unless all acoustic modes are cut-off. So it makes sense to use the acoustic modes as a “complete” basis to construct a general solution.
- Trailing vortices in boundary layer.
- The relevance of the spatial instability.
- The (related) question of the limit of $h \to 0$ (the Ingard-Myers limit): the boundary condition with $U_{\text{wall}} = 0$ changes to an equivalent boundary condition for U_{wall} finite.

$$\mathrm{i}\omega Z \tilde{v} = \left(\mathrm{i}\omega + U_{\text{wall}} \frac{\partial}{\partial x}\right) \tilde{p}$$

How physical is this?

Interim conclusions

- The contribution from the branch cut and its associated pole is very minor unless all acoustic modes are cut-off. So it makes sense to use the acoustic modes as a “complete” basis to construct a general solution.
- Trailing vortices in boundary layer.
- The relevance of the spatial instability.
- The (related) question of the limit of $h \to 0$ (the Ingard-Myers limit): the boundary condition with $U_{\text{wall}} = 0$ changes to an equivalent boundary condition for U_{wall} finite.

$$\mathrm{i}\omega Z \tilde{v} = \left(\mathrm{i}\omega + U_{\text{wall}} \frac{\partial}{\partial x}\right) \tilde{p}$$

How physical is this?

Interim conclusions

- The contribution from the branch cut and its associated pole is very minor unless all acoustic modes are cut-off. So it makes sense to use the acoustic modes as a "complete" basis to construct a general solution.
- Trailing vortices in boundary layer.
- The relevance of the spatial instability.
- The (related) question of the limit of $h \to 0$ (the Ingard-Myers limit): the boundary condition with $U_{\text{wall}} = 0$ changes to an equivalent boundary condition for U_{wall} finite.

$$\mathrm{i}\omega Z\tilde{v} = \left(\mathrm{i}\omega + U_{\text{wall}}\frac{\partial}{\partial x}\right)\tilde{p}$$

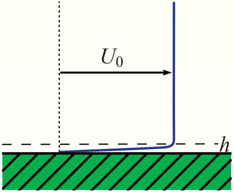

How physical is this?

The Ingard-Myers boundary condition

- In any reality, $\exists$(perturbations) exciting other (complex) frequencies†
- If $h < h_c$, they include an **absolute instability** $\sim \mathrm{e}^{\mathrm{i}\omega^* t}$ (group velocity $= 0$), while growth rate $-\mathrm{Im}(\omega^*) \to \infty$ for $h \to 0$.
- This makes the problem *ill-posed* in time (Brambley).

†If the problem is forced to be *time-harmonic*, there are no other than spatial instabilities.

The Ingard-Myers boundary condition

- In any reality, ∃(perturbations) exciting other (complex) frequencies†
- If $h < h_c$, they include an **absolute instability** $\sim \mathrm{e}^{\mathrm{i}\omega^* t}$ (group velocity $= 0$), while growth rate $-\mathrm{Im}(\omega^*) \to \infty$ for $h \to 0$.

- This makes the problem *ill-posed* in time (Brambley).

†If the problem is forced to be *time-harmonic*, there are no other than spatial instabilities.

The Ingard-Myers boundary condition

- In any reality, $\exists$(perturbations) exciting other (complex) frequencies†
- If $h < h_c$, they include an **absolute instability** $\sim e^{i\omega^* t}$ (group velocity $= 0$), while growth rate $-\mathrm{Im}(\omega^*) \to \infty$ for $h \to 0$.

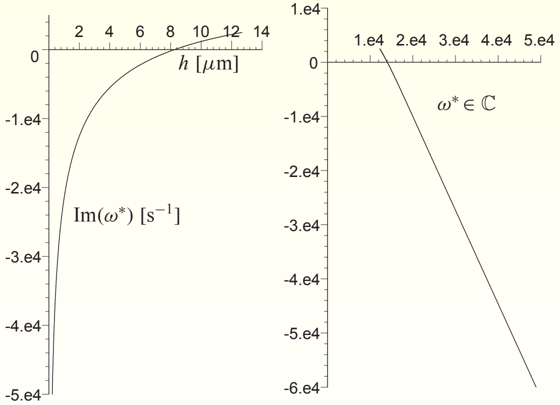

Absolute instability ω^* for varying h

- This makes the problem *ill-posed* in time (Brambley).

†If the problem is forced to be *time-harmonic*, there are no other than spatial instabilities.

The Ingard-Myers boundary condition

- In any reality, ∃(perturbations) exciting other (complex) frequencies[†]
- If $h < h_c$, they include an **absolute instability** $\sim \mathrm{e}^{\mathrm{i}\omega^* t}$ (group velocity $= 0$), while growth rate $-\mathrm{Im}(\omega^*) \to \infty$ for $h \to 0$.

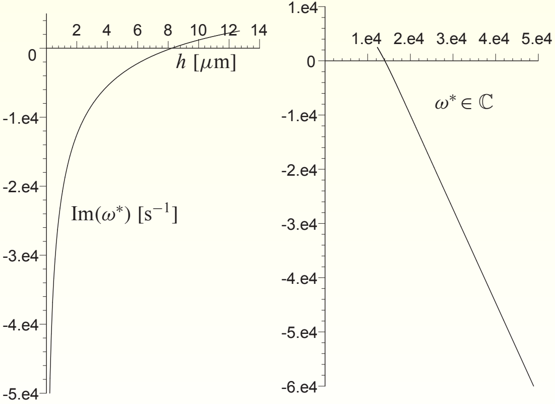

Absolute instability ω^* for varying h

- This makes the problem *ill-posed* in time (Brambley).

[†]If the problem is forced to be *time-harmonic*, there are no other than spatial instabilities.

Condition for absolute instability

For mass-spring-damper impedance

$$Z = R + \mathrm{i}\omega m + (\mathrm{i}\omega)^{-1}K, \quad K = \rho_0 c_0^2/L$$

dimensional arguments reveil that

$$h_c = \left(\frac{\rho_0 U_\infty}{R}\right)^2 U_\infty \sqrt{\frac{m}{K}} \times F\left(\frac{\sqrt{mK}}{\rho_0 U_\infty}, \frac{R}{\rho_0 U_\infty}\right) \simeq \frac{1}{4}\left(\frac{\rho_0 U_\infty}{R}\right)^2 U_\infty \sqrt{\frac{m}{K}}$$

Condition for absolute instability

For mass-spring-damper impedance

$$Z = R + \mathrm{i}\omega m + (\mathrm{i}\omega)^{-1} K, \qquad K = \rho_0 c_0^2 / L$$

dimensional arguments reveil that

$$h_c = \left(\frac{\rho_0 U_\infty}{R}\right)^2 U_\infty \sqrt{\frac{m}{K}} \times F\left(\frac{\sqrt{mK}}{\rho_0 U_\infty}, \frac{R}{\rho_0 U_\infty}\right) \simeq \frac{1}{4}\left(\frac{\rho_0 U_\infty}{R}\right)^2 U_\infty \sqrt{\frac{m}{K}}$$

Condition for absolute instability

For mass-spring-damper impedance

$$Z = R + \mathrm{i}\omega m + (\mathrm{i}\omega)^{-1} K, \quad K = \rho_0 c_0^2 / L$$

dimensional arguments reveil that

$$h_c = \Big(\frac{\rho_0 U_\infty}{R}\Big)^2 U_\infty \sqrt{\frac{m}{K}} \times F\Big(\frac{\sqrt{mK}}{\rho_0 U_\infty}, \frac{R}{\rho_0 U_\infty}\Big) \simeq \frac{1}{4}\Big(\frac{\rho_0 U_\infty}{R}\Big)^2 U_\infty \sqrt{\frac{m}{K}}$$

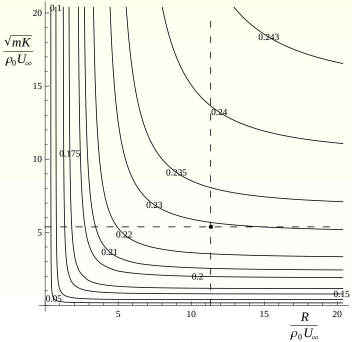

With $R = 2\rho_0 c_0$, $L = 3.5$ cm, $m/\rho_0 = 32$ mm, $U_\infty = 60$ m/s,
this is very, very small: $h_c = 10.5\mu$m *(less than a hair!)*.

Condition for absolute instability

For mass-spring-damper impedance

$$Z = R + \mathrm{i}\omega m + (\mathrm{i}\omega)^{-1}K, \quad K = \rho_0 c_0^2/L$$

dimensional arguments reveil that

$$h_c = \Big(\frac{\rho_0 U_\infty}{R}\Big)^2 U_\infty \sqrt{\frac{m}{K}} \times F\Big(\frac{\sqrt{mK}}{\rho_0 U_\infty}, \frac{R}{\rho_0 U_\infty}\Big) \simeq \frac{1}{4}\Big(\frac{\rho_0 U_\infty}{R}\Big)^2 U_\infty \sqrt{\frac{m}{K}}$$

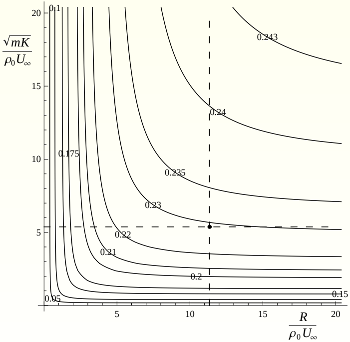

With $R = 2\rho_0 c_0$, $L = 3.5$ cm, $m/\rho_0 = 32$ mm, $U_\infty = 60$ m/s,
this is very, very small: $h_c = 10.5\mu$m *(less than a hair!)*.

Outline

Trailing vorticity from mass source

Compressible Euler equations with mass source and force

$$\frac{\partial \rho}{\partial t} + \nabla\cdot(\rho\boldsymbol{v}) = \rho Q, \qquad \rho\frac{\partial \boldsymbol{v}}{\partial t} + \rho(\boldsymbol{v}\cdot\nabla\boldsymbol{v}) + \nabla p = \rho\boldsymbol{F}$$

In barotropic fluid and $\boldsymbol{\omega} = \nabla\times\boldsymbol{v}$:

$$\rho\left(\frac{\partial}{\partial t} + \boldsymbol{v}\cdot\nabla\right)\left(\frac{\boldsymbol{\omega}}{\rho}\right) = \boldsymbol{\omega}\cdot\nabla\boldsymbol{v} - \frac{\boldsymbol{\omega}}{\rho}Q + \nabla\times\boldsymbol{F}$$

Vorticity is only produced by non-conservative force field $\boldsymbol{F}$, or by mass source Q in mean vorticity.

Trailing vorticity from mass source

Compressible Euler equations with mass source and force

$$\frac{\partial \rho}{\partial t} + \nabla\cdot(\rho \boldsymbol{v}) = \rho Q, \qquad \rho \frac{\partial \boldsymbol{v}}{\partial t} + \rho(\boldsymbol{v}\cdot\nabla \boldsymbol{v}) + \nabla p = \rho \boldsymbol{F}$$

In barotropic fluid and $\boldsymbol{\omega} = \nabla \times \boldsymbol{v}$:

$$\rho\left(\frac{\partial}{\partial t} + \boldsymbol{v}\cdot\nabla\right)\left(\frac{\boldsymbol{\omega}}{\rho}\right) = \boldsymbol{\omega}\cdot\nabla \boldsymbol{v} - \frac{\boldsymbol{\omega}}{\rho} Q + \nabla \times \boldsymbol{F}$$

Vorticity is only produced by non-conservative force field $\boldsymbol{F}$, or by mass source Q in mean vorticity.

Trailing vorticity from mass source

Compressible Euler equations with mass source and force

$$\frac{\partial \rho}{\partial t} + \nabla \cdot (\rho \boldsymbol{v}) = \rho Q, \qquad \rho \frac{\partial \boldsymbol{v}}{\partial t} + \rho (\boldsymbol{v} \cdot \nabla \boldsymbol{v}) + \nabla p = \rho \boldsymbol{F}$$

In barotropic fluid and $\boldsymbol{\omega} = \nabla \times \boldsymbol{v}$:

$$\rho \left(\frac{\partial}{\partial t} + \boldsymbol{v} \cdot \nabla \right) \left(\frac{\boldsymbol{\omega}}{\rho} \right) = \boldsymbol{\omega} \cdot \nabla \boldsymbol{v} - \frac{\boldsymbol{\omega}}{\rho} Q + \nabla \times \boldsymbol{F}$$

Vorticity is only produced by non-conservative force field $\boldsymbol{F}$, or by mass source Q in mean vorticity.

Trailing vorticity from mass source

In 2D linear shear flow

If $U = U_0 + \sigma y, \quad \hat{\varphi} = 0$ and harmonic point source $Q = \delta(x, y)\,\mathrm{e}^{\mathrm{i}\omega t}$, we have in the incompressible limit for z-component $\boldsymbol{\omega}_z = \chi$

$$\left(\mathrm{i}\omega + U\frac{\partial}{\partial x}\right)\hat{\chi} = \frac{\sigma}{\rho_0}\delta(x, y)$$

with remarkably simple solution

$$\hat{\chi} = \frac{\sigma}{\rho_0 U_0} H(x)\,\mathrm{e}^{-\mathrm{i}k_0 y}\,\delta(y), \qquad k_0 = \frac{\omega}{U_0}$$

Trailing vorticity from a mass source in shear flow.
Hydrodynamic wavenumber k_0.

Trailing vorticity from mass source

In 2D linear shear flow

If $U = U_0 + \sigma y$, $\hat{\varphi} = 0$ and harmonic point source $Q = \delta(x, y)\, \mathrm{e}^{\mathrm{i}\omega t}$, we have in the incompressible limit for z-component $\boldsymbol{\omega}_z = \chi$

$$\left(\mathrm{i}\omega + U\frac{\partial}{\partial x}\right)\hat{\chi} = \frac{\sigma}{\rho_0}\delta(x, y)$$

with remarkably simple solution

$$\hat{\chi} = \frac{\sigma}{\rho_0 U_0} H(x)\, \mathrm{e}^{-\mathrm{i}k_0 y}\, \delta(y), \quad k_0 = \frac{\omega}{U_0}$$

Trailing vorticity from a mass source in shear flow.
Hydrodynamic wavenumber k_0.

Trailing vorticity from mass source

In 2D linear shear flow

If $U = U_0 + \sigma y, \quad \hat{\varphi} = 0$ and harmonic point source $Q = \delta(x, y)\,\mathrm{e}^{\mathrm{i}\omega t}$, we have in the incompressible limit for z-component $\boldsymbol{\omega}_z = \chi$

$$\left(\mathrm{i}\omega + U\frac{\partial}{\partial x}\right)\hat{\chi} = \frac{\sigma}{\rho_0}\delta(x, y)$$

with remarkably simple solution

$$\hat{\chi} = \frac{\sigma}{\rho_0 U_0} H(x)\,\mathrm{e}^{-\mathrm{i}k_0 y}\,\delta(y), \qquad k_0 = \frac{\omega}{U_0}$$

Trailing vorticity from a mass source in shear flow.
Hydrodynamic wavenumber k_0.

Examples. $\omega = 8, U' = \sigma = 6$

free field

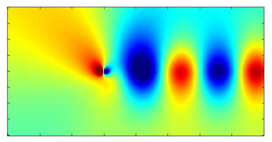

pressure

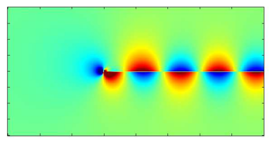

u-velocity

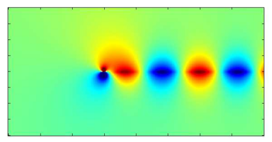

v-velocity

Examples. $\omega = 8, U' = \sigma = 6$

free field

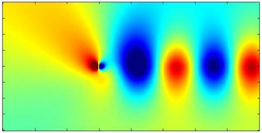

pressure

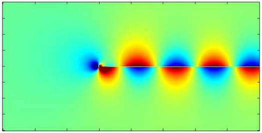

u-velocity

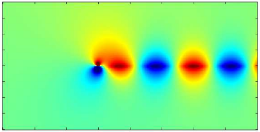

v-velocity

hard wall

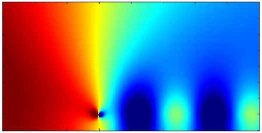

pressure

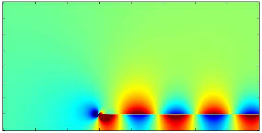

u-velocity

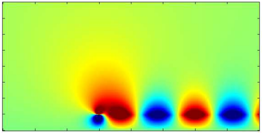

v-velocity

Examples. $\omega = 8$, $U' = \sigma = 6$

free field

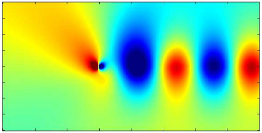

pressure

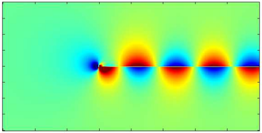

u-velocity

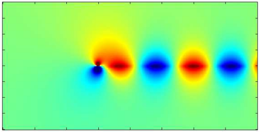

v-velocity

hard wall

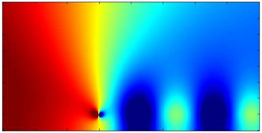

pressure

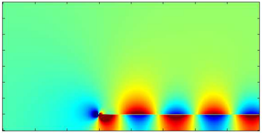

u-velocity

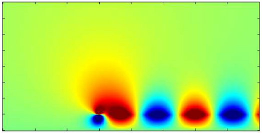

v-velocity

impedance wall $Z = 4 - 2\mathrm{i}$

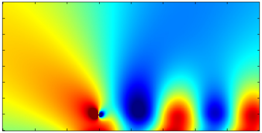

pressure

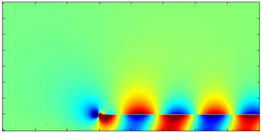

u-velocity

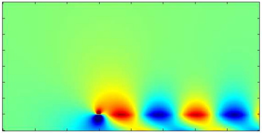

v-velocity

Scattering at hard-soft transition (by Wiener-Hopf)

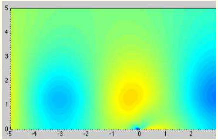

pressure

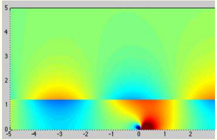

u-velocity

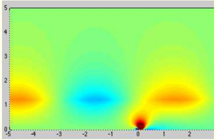

v-velocity

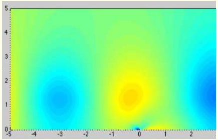

pressure

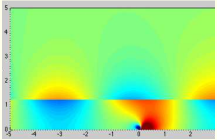

u-velocity

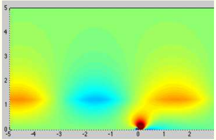

v-velocity

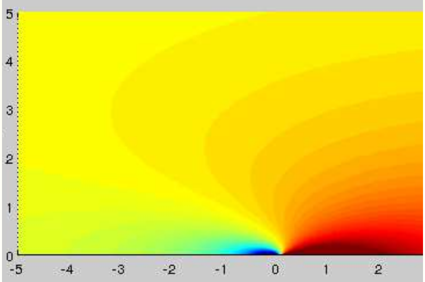

far field (acoustic) pressure

$U' < \omega$ is essential. Field diverges for $U' > \omega$, requiring a finite BL.

Interim conclusions

- A complete solution, including the branch cut contributions, is rarely possible. It is shown that the Pridmore-Brown modes dominate and can be used as approximate basis.
- Thin boundary layer along impedance wall becomes absolute unstable, with infinite growth rate for vanishing boundary layer (ill-posed). A finite boundary layer regularises this.
- A mass source in shear flow produces trailing vortices. These may scatter and radiate into sound at hard-soft transitions. The behaviour is radically different for $\omega \gtrless U'$.

Interim conclusions

- A complete solution, including the branch cut contributions, is rarely possible. It is shown that the Pridmore-Brown modes dominate and can be used as approximate basis.
- Thin boundary layer along impedance wall becomes absolute unstable, with infinite growth rate for vanishing boundary layer (ill-posed). A finite boundary layer regularises this.
- A mass source in shear flow produces trailing vortices. These may scatter and radiate into sound at hard-soft transitions. The behaviour is radically different for $\omega \gtrless U'$.

Interim conclusions

- A complete solution, including the branch cut contributions, is rarely possible. It is shown that the Pridmore-Brown modes dominate and can be used as approximate basis.
- Thin boundary layer along impedance wall becomes absolute unstable, with infinite growth rate for vanishing boundary layer (ill-posed). A finite boundary layer regularises this.
- A mass source in shear flow produces trailing vortices. These may scatter and radiate into sound at hard-soft transitions. The behaviour is radically different for $\omega \gtrless U'$.

Outline

Mode matching: motivation

- APU is typically a straight duct with strong (radial) temperature and mean flow gradients, and sectioned, varying boundary conditions.

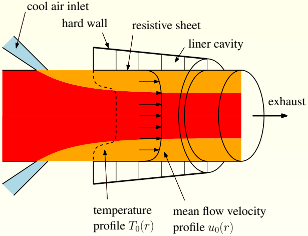

- "General" solution per section by sum over modes

$$p_m(r,x) = \sum_{\mu=1}^{\infty} \left[A_{m\mu}^{+} P_{m\mu}^{+}(r)\, \mathrm{e}^{\mathrm{i}k_{m\mu}^{+}x} + A_{m\mu}^{-} P_{m\mu}^{-}(r)\, \mathrm{e}^{\mathrm{i}k_{m\mu}^{-}x} \right]$$

Typically suited for mode-matching approach.

- New efficient and accurate **Mode-Matching method** based on **exact** integrals of Pridmore-Brown modes.

Mode matching: motivation

- APU is typically a straight duct with strong (radial) temperature and mean flow gradients, and sectioned, varying boundary conditions.

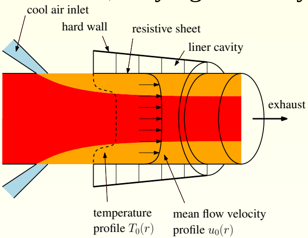

- "General" solution per section by sum over modes

$$p_m(r,x) = \sum_{\mu=1}^{\infty} \left[A^{+}_{m\mu} P^{+}_{m\mu}(r)\, \mathrm{e}^{\mathrm{i}k^{+}_{m\mu}x} + A^{-}_{m\mu} P^{-}_{m\mu}(r)\, \mathrm{e}^{\mathrm{i}k^{-}_{m\mu}x} \right]$$

  Typically suited for mode-matching approach.

- New efficient and accurate **Mode-Matching method** based on **exact** integrals of Pridmore-Brown modes.

Mode matching: motivation

- APU is typically a straight duct with strong (radial) temperature and mean flow gradients, and sectioned, varying boundary conditions.

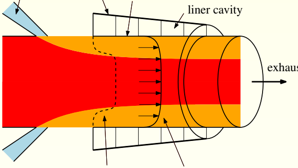

- "General" solution per section by sum over modes

$$p_m(r,x) = \sum_{\mu=1}^{\infty} \left[A^{+}_{m\mu} P^{+}_{m\mu}(r)\, \mathrm{e}^{\mathrm{i}k^{+}_{m\mu}x} + A^{-}_{m\mu} P^{-}_{m\mu}(r)\, \mathrm{e}^{\mathrm{i}k^{-}_{m\mu}x} \right]$$

  Typically suited for mode-matching approach.

- New efficient and accurate **Mode-Matching method** based on **exact** integrals of Pridmore-Brown modes.

Mode-Matching Basics

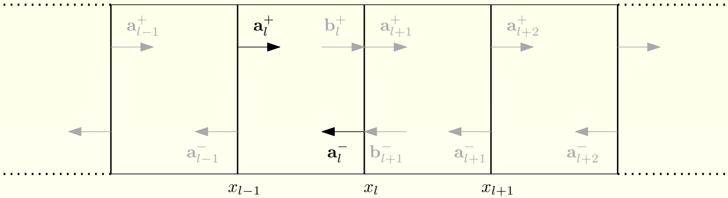

Total field in segment l: sum of left- and right-running waves

$$p_l(x,r) = \sum_{\mu=1}^{\mu^{\max}} \left(a^+_{l,\mu} P^+_{l,\mu}(r)\, \mathrm{e}^{\mathrm{i}k^+_{l,\mu}(x-x_{l-1})} + a^-_{l,\mu} P^-_{l,\mu}(r)\, \mathrm{e}^{\mathrm{i}k^-_{l,\mu}(x-x_l)} \right)$$

(same for velocity)

Mode-Matching Basics

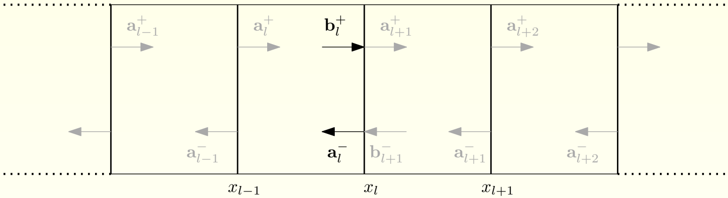

At the interface at $x = x_l$:

$$p_l(r) = \sum_{\mu=1}^{\mu^{\max}} \left(b_{l,\mu}^+ P_{l,\mu}^+(r) + a_{l,\mu}^- P_{l,\mu}^-(r) \right).$$

(same for velocity)

Classical mode-matching

Mode-Matching Basics

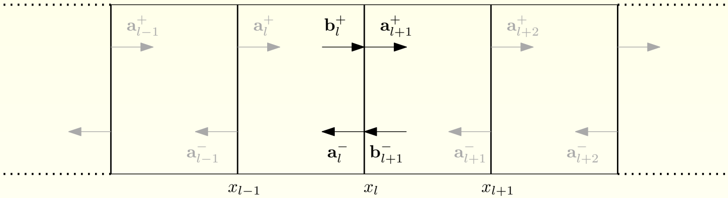

Continuity of pressure at $x = x_l$ leads to

$$p_l(x_l, r) = p_{l+1}(x_l, r)$$

Mode-Matching Basics

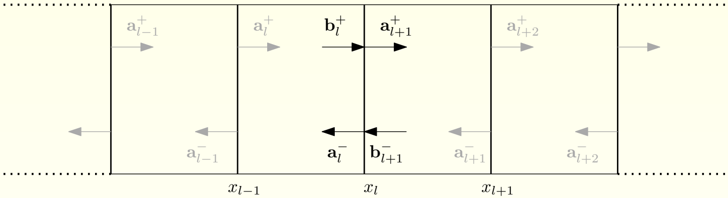

Continuity of pressure at $x = x_l$ leads to

$$\sum_{\mu=1}^{\mu^{\max}} \left(b^+_{l,\mu} \left(P^+_{l,\mu}, \Psi_\nu \right) + a^-_{l,\mu} \left(P^-_{l,\mu}, \Psi_\nu \right) \right)$$

$$= \sum_{\mu=1}^{\mu^{\max}} \left(a^+_{l+1,\mu} \left(P^+_{l+1,\mu}, \Psi_\nu \right) + b^-_{l+1,\mu} \left(P^-_{l+1,\mu}, \Psi_\nu \right) \right)$$

Mode-Matching Basics

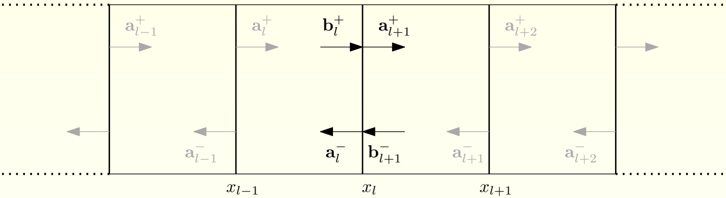

inner products with suitable test functions Ψ_ν, e.g. $= J_m(\alpha_\nu r)$

$$\sum_{\mu=1}^{\mu^{\max}} \left(b_{l,\mu}^+ (P_{l,\mu}^+, \Psi_\nu) + a_{l,\mu}^- (P_{l,\mu}^-, \Psi_\nu) \right)$$

$$= \sum_{\mu=1}^{\mu^{\max}} \left(a_{l+1,\mu}^+ (P_{l+1,\mu}^+, \Psi_\nu) + b_{l+1,\mu}^- (P_{l+1,\mu}^-, \Psi_\nu) \right)$$

Mode-Matching Basics

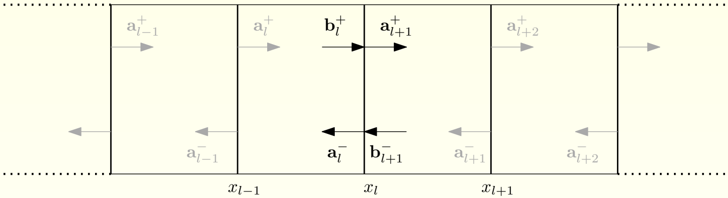

inner products with suitable test functions Ψ_ν, e.g. $= J_m(\alpha_\nu r)$

$$\sum_{\mu=1}^{\mu^{\max}} \left(b^+_{l,\mu} (P^+_{l,\mu}, \Psi_\nu) + a^-_{l,\mu} (P^-_{l,\mu}, \Psi_\nu) \right)$$

$$= \sum_{\mu=1}^{\mu^{\max}} \left(a^+_{l+1,\mu} (P^+_{l+1,\mu}, \Psi_\nu) + b^-_{l+1,\mu} (P^-_{l+1,\mu}, \Psi_\nu) \right)$$

Similar for continuity of axial velocity.

Mode-Matching Basics

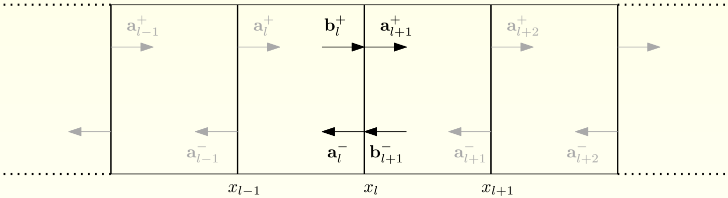

Results in linear system to be solved

$$\begin{bmatrix} \vec{A}^+ & \vec{A}^- \\ \vec{C}^+ & \vec{C}^- \end{bmatrix} \begin{bmatrix} \vec{b}_l^+ \\ \vec{a}_l^- \end{bmatrix} = \begin{bmatrix} \vec{B}^+ & \vec{B}^- \\ \vec{D}^+ & \vec{D}^- \end{bmatrix} \begin{bmatrix} \vec{a}_{l+1}^+ \\ \vec{b}_{l+1}^- \end{bmatrix}.$$

Computing inner products

Matrix entries are inner products

$$A^{\pm}_{\nu\mu} = (P^{\pm}_{l,\mu}, \Psi_\nu) = \int_0^1 P^{\pm}_{l,\mu}(r)\Psi_\nu(r) r \,\mathrm{d}r$$

Note that for non-uniform flow:

- $P^{\pm}_{l,\mu}$ is determined numerically
- All inner-products have to be determined at all interfaces by quadrature
- $P^{\pm}_{l,\mu}$ and Ψ_ν are oscillatory $\Rightarrow$ numerical problems

Problem

Computing inner products numerically is expensive / less accurate

Computing inner products

Matrix entries are inner products

$$A^{\pm}_{\nu\mu} = (P^{\pm}_{l,\mu}, \Psi_\nu) = \int_0^1 P^{\pm}_{l,\mu}(r)\Psi_\nu(r)r\,\mathrm{d}r$$

Note that for non-uniform flow:

- $P^{\pm}_{l,\mu}$ is determined numerically
- All inner-products have to be determined at all interfaces by quadrature
- $P^{\pm}_{l,\mu}$ and Ψ_ν are oscillatory $\Rightarrow$ numerical problems

Problem

Computing inner products numerically is expensive / less accurate

Computing inner products

Matrix entries are inner products

$$A^{\pm}_{\nu\mu} = (P^{\pm}_{l,\mu}, \Psi_\nu) = \int_0^1 P^{\pm}_{l,\mu}(r)\Psi_\nu(r) r \, \mathrm{d}r$$

Note that for non-uniform flow:

- $P^{\pm}_{l,\mu}$ is determined numerically
- All inner-products have to be determined at all interfaces by quadrature
- $P^{\pm}_{l,\mu}$ and Ψ_ν are oscillatory $\Rightarrow$ numerical problems

Problem

Computing inner products numerically is expensive / less accurate

Computing inner products

Matrix entries are inner products

$$A^{\pm}_{\nu\mu} = (P^{\pm}_{l,\mu}, \Psi_\nu) = \int_0^1 P^{\pm}_{l,\mu}(r)\Psi_\nu(r) r \, \mathrm{d}r$$

Note that for non-uniform flow:

- $P^{\pm}_{l,\mu}$ is determined numerically
- All inner-products have to be determined at all interfaces by quadrature
- $P^{\pm}_{l,\mu}$ and Ψ_ν are oscillatory $\Rightarrow$ numerical problems

Problem

Computing inner products numerically is expensive / less accurate

Computing inner products

Matrix entries are inner products

$$A^{\pm}_{\nu\mu} = (P^{\pm}_{l,\mu}, \Psi_\nu) = \int_0^1 P^{\pm}_{l,\mu}(r)\Psi_\nu(r) r \, \mathrm{d}r$$

Note that for non-uniform flow:

- $P^{\pm}_{l,\mu}$ is determined numerically
- All inner-products have to be determined at all interfaces by quadrature
- $P^{\pm}_{l,\mu}$ and Ψ_ν are oscillatory $\Rightarrow$ numerical problems

Problem

Computing inner products numerically is expensive / less accurate

Computing inner products

Matrix entries are inner products

$$A^{\pm}_{\nu\mu} = (P^{\pm}_{l,\mu}, \Psi_\nu) = \int_0^1 P^{\pm}_{l,\mu}(r)\Psi_\nu(r) r \, \mathrm{d}r$$

Note that for non-uniform flow:

- $P^{\pm}_{l,\mu}$ is determined numerically
- All inner-products have to be determined at all interfaces by quadrature
- $P^{\pm}_{l,\mu}$ and Ψ_ν are oscillatory $\Rightarrow$ numerical problems

Problem

Computing inner products numerically is expensive / less accurate

Computing inner products

Matrix entries are inner products

$$A^{\pm}_{\nu\mu} = (P^{\pm}_{l,\mu}, \Psi_\nu) = \int_0^1 P^{\pm}_{l,\mu}(r)\Psi_\nu(r) r \,\mathrm{d}r$$

Note that for non-uniform flow:

- $P^{\pm}_{l,\mu}$ is determined numerically
- All inner-products have to be determined at all interfaces by quadrature
- $P^{\pm}_{l,\mu}$ and Ψ_ν are oscillatory $\Rightarrow$ numerical problems

Problem

Computing inner products numerically is expensive / less accurate

Central question

Can we find closed-form expressions for the inner-product?

Computing inner products

Matrix entries are inner products

$$A^{\pm}_{\nu\mu} = (P^{\pm}_{l,\mu}, \Psi_\nu) = \int_0^1 P^{\pm}_{l,\mu}(r)\Psi_\nu(r) r \, \mathrm{d}r$$

Note that for non-uniform flow:

- $P^{\pm}_{l,\mu}$ is determined numerically
- All inner-products have to be determined at all interfaces by quadrature
- $P^{\pm}_{l,\mu}$ and Ψ_ν are oscillatory $\Rightarrow$ numerical problems

Problem

Computing inner products numerically is expensive / less accurate

Central question

Can we find closed-form expressions for the inner-product? No

Computing inner products

Matrix entries are inner products

$$A^{\pm}_{\nu\mu} = (P^{\pm}_{l,\mu}, \Psi_\nu) = \int_0^1 P^{\pm}_{l,\mu}(r)\Psi_\nu(r)r \,\mathrm{d}r$$

Note that for non-uniform flow:

- $P^{\pm}_{l,\mu}$ is determined numerically
- All inner-products have to be determined at all interfaces by quadrature
- $P^{\pm}_{l,\mu}$ and Ψ_ν are oscillatory $\Rightarrow$ numerical problems

Problem

Computing inner products numerically is expensive / less accurate

Central question

Can we find closed-form expressions for *other* ‘inner-product’?

Computing inner products

Matrix entries are inner products

$$A^{\pm}_{\nu\mu} = (P^{\pm}_{l,\mu}, \Psi_\nu) = \int_0^1 P^{\pm}_{l,\mu}(r)\Psi_\nu(r)r \,\mathrm{d}r$$

Note that for non-uniform flow:

- $P^{\pm}_{l,\mu}$ is determined numerically
- All inner-products have to be determined at all interfaces by quadrature
- $P^{\pm}_{l,\mu}$ and Ψ_ν are oscillatory $\Rightarrow$ numerical problems

Problem

Computing inner products numerically is expensive / less accurate

Central question

Can we find closed-form expressions for *other* ‘inner-product’? Yes!

From Classical to a New Mode-matching method

Summary of new matching method

Classical (CMM)	$\rightarrow$	**New (NMM)** mode-matching
(P_μ, Ψ_ν)	$\rightarrow$	$\langle \boldsymbol{F}_\mu, \boldsymbol{\Psi}_\nu \rangle$
$= \int_0^1 P_\mu \Psi_\nu r \,\mathrm{d}r$	$\rightarrow$	$= \int_0^1 \big[w_1 P_\mu P_\nu + w_2 U_\mu P_\nu + w_3 (V_\mu V_\nu + W_\mu W_\nu) \big] r \,\mathrm{d}r$
quadrature	$\rightarrow$	$= \dfrac{\mathrm{i}}{k_\mu - k_\nu} \left[\dfrac{P_\nu V_\mu - V_\nu P_\mu}{\Omega_\nu} \right]_{r=1}$
with $\Psi_\nu = J_m(\alpha_\nu r)$		with $\boldsymbol{\Psi}_\nu = \boldsymbol{F}_\nu$, $\quad \boldsymbol{F}_\mu = [P_\mu, U_\mu, V_\mu, W_\mu]$

Summary of new matching method

Classical (CMM)	$\rightarrow$	**New (NMM)** mode-matching
(P_μ, Ψ_ν)	$\rightarrow$	$\langle \boldsymbol{F}_\mu, \boldsymbol{\Psi}_\nu \rangle$
$= \int_0^1 P_\mu \Psi_\nu r \,\mathrm{d}r$	$\rightarrow$	$= \int_0^1 \big[w_1 P_\mu P_\nu + w_2 U_\mu P_\nu + w_3 (V_\mu V_\nu + W_\mu W_\nu) \big] r \,\mathrm{d}r$
quadrature	$\rightarrow$	$= \dfrac{\mathrm{i}}{k_\mu - k_\nu} \left[\dfrac{P_\nu V_\mu - V_\nu P_\mu}{\Omega_\nu} \right]_{r=1}$
with $\Psi_\nu = J_m(\alpha_\nu r)$		with $\boldsymbol{\Psi}_\nu = \boldsymbol{F}_\nu, \quad \boldsymbol{F}_\mu = [P_\mu, U_\mu, V_\mu, W_\mu]$

Summary of new matching method

Classical (CMM)	$\rightarrow$	**New (NMM)** mode-matching
(P_μ, Ψ_ν)	$\rightarrow$	$\langle \boldsymbol{F}_\mu, \boldsymbol{\Psi}_\nu \rangle$
$= \int_0^1 P_\mu \Psi_\nu r \, \mathrm{d}r$	$\rightarrow$	$= \int_0^1 \big[w_1 P_\mu P_\nu + w_2 U_\mu P_\nu + w_3 (V_\mu V_\nu + W_\mu W_\nu) \big] r \, \mathrm{d}r$
quadrature	$\rightarrow$	$= \dfrac{\mathrm{i}}{k_\mu - k_\nu} \left[\dfrac{P_\nu V_\mu - V_\nu P_\mu}{\Omega_\nu} \right]_{r=1}$
with $\Psi_\nu = J_m(\alpha_\nu r)$		with $\boldsymbol{\Psi}_\nu = \boldsymbol{F}_\nu, \quad \boldsymbol{F}_\mu = [P_\mu, U_\mu, V_\mu, W_\mu]$

Summary of new matching method

Classical (CMM)	$\rightarrow$	**New (NMM)** mode-matching
(P_μ, Ψ_ν)	$\rightarrow$	$\langle \boldsymbol{F}_\mu, \boldsymbol{\Psi}_\nu \rangle$
$= \int_0^1 P_\mu \Psi_\nu r \,\mathrm{d}r$	$\rightarrow$	$= \int_0^1 \big[w_1 P_\mu P_\nu + w_2 U_\mu P_\nu + w_3 (V_\mu V_\nu + W_\mu W_\nu) \big] r \,\mathrm{d}r$
quadrature	$\rightarrow$	$= \dfrac{\mathrm{i}}{k_\mu - k_\nu} \left[\dfrac{P_\nu V_\mu - V_\nu P_\mu}{\Omega_\nu} \right]_{r=1}$
with $\Psi_\nu = J_m(\alpha_\nu r)$		with $\boldsymbol{\Psi}_\nu = \boldsymbol{F}_\nu$, $\quad \boldsymbol{F}_\mu = [P_\mu, U_\mu, V_\mu, W_\mu]$
expensive less accurate	$\rightarrow$	cheap accurate

Closed form integrals of 2D eigenmodes

Prototype example of *Generalised Pridmore-Brown* : Helmholtz equation

$$\phi\left(\nabla^2\psi + \beta^2\psi\right) = 0$$

$$\psi\left(\nabla^2\phi + \alpha^2\phi\right) = 0$$

on arbitrarily shaped cross-section $\mathcal{A}$

Subtract and integrate over $\mathcal{A}$

$$(\alpha^2 - \beta^2)\iint_{\mathcal{A}} \phi\psi \,\mathrm{d}S \;= \overset{\text{GAUSS}}{\downarrow}$$

2D inner-product for Helmholtz eigenfunctions

$$\langle\!\langle \phi, \psi \rangle\!\rangle = \frac{1}{\alpha^2 - \beta^2}\int_{\Gamma} (\phi\nabla\psi\cdot\boldsymbol{n} - \psi\nabla\phi\cdot\boldsymbol{n})\mathrm{d}\ell,$$

for arbitrary boundary conditions on ϕ and ψ

What if $\alpha = \beta$ and $\phi = \psi$? Something similar.

Closed form integrals of 2D eigenmodes

Prototype example of *Generalised Pridmore-Brown* : Helmholtz equation

$$\phi\left(\nabla^2\psi + \beta^2\psi\right) = 0$$
$$\psi\left(\nabla^2\phi + \alpha^2\phi\right) = 0$$

on arbitrarily shaped cross-section $\mathcal{A}$

Subtract and integrate over $\mathcal{A}$

$$(\alpha^2 - \beta^2)\iint_{\mathcal{A}} \phi\psi \, \mathrm{d}S \overset{\text{GAUSS}}{=}$$

2D inner-product for Helmholtz eigenfunctions

$$\langle\langle \phi, \psi \rangle\rangle = \frac{1}{\alpha^2 - \beta^2}\int_{\Gamma}(\phi\nabla\psi\cdot\boldsymbol{n} - \psi\nabla\phi\cdot\boldsymbol{n})\mathrm{d}\ell,$$

for arbitrary boundary conditions on ϕ and ψ

What if $\alpha = \beta$ and $\phi = \psi$? Something similar.

Closed form integrals of 2D eigenmodes

Prototype example of *Generalised Pridmore-Brown* : Helmholtz equation

$$\phi\left(\nabla^2\psi + \beta^2\psi\right) = 0$$
$$\psi\left(\nabla^2\phi + \alpha^2\phi\right) = 0$$

on arbitrarily shaped cross-section $\mathcal{A}$

Subtract and integrate over $\mathcal{A}$

GAUSS

$$(\alpha^2 - \beta^2)\iint_{\mathcal{A}} \phi\psi\,\mathrm{d}S = $$

2D inner-product for Helmholtz eigenfunctions

$$\langle\!\langle \phi, \psi \rangle\!\rangle = \frac{1}{\alpha^2 - \beta^2}\int_{\Gamma}(\phi\nabla\psi\cdot\boldsymbol{n} - \psi\nabla\phi\cdot\boldsymbol{n})\mathrm{d}\ell,$$

for arbitrary boundary conditions on ϕ and ψ

What if $\alpha = \beta$ and $\phi = \psi$? Something similar.

Closed form integrals of 2D eigenmodes

Prototype example of *Generalised Pridmore-Brown* : Helmholtz equation

$$\phi\left(\nabla^2\psi+\beta^2\psi\right)=0$$
$$\psi\left(\nabla^2\phi+\alpha^2\phi\right)=0$$

on arbitrarily shaped cross-section $\mathcal{A}$
Subtract and integrate over $\mathcal{A}$

$$(\alpha^2-\beta^2)\iint_{\mathcal{A}}\phi\psi\,\mathrm{d}S \;=\; \overset{\text{GAUSS}}{\iint_{\mathcal{A}}}(\phi\nabla^2\psi-\psi\nabla^2\phi)\,\mathrm{d}S$$

2D inner-product for Helmholtz eigenfunctions

$$\langle\langle\phi,\psi\rangle\rangle=\frac{1}{\alpha^2-\beta^2}\int_{\Gamma}(\phi\nabla\psi\cdot\boldsymbol{n}-\psi\nabla\phi\cdot\boldsymbol{n})\mathrm{d}\ell,$$

for arbitrary boundary conditions on ϕ and ψ

What if $\alpha=\beta$ and $\phi=\psi$? Something similar.

Closed form integrals of 2D eigenmodes

Prototype example of *Generalised Pridmore-Brown* : Helmholtz equation

$$\phi\left(\nabla^2\psi + \beta^2\psi\right) = 0$$
$$\psi\left(\nabla^2\phi + \alpha^2\phi\right) = 0$$

on arbitrarily shaped cross-section $\mathcal{A}$
Subtract and integrate over $\mathcal{A}$

GAUSS

$$(\alpha^2 - \beta^2)\iint_{\mathcal{A}} \phi\psi \, \mathrm{d}S = \iint_{\mathcal{A}} (\phi\nabla^2\psi - \psi\nabla^2\phi)\, \mathrm{d}S$$

2D inner-product for Helmholtz eigenfunctions

$$\langle\!\langle \phi, \psi \rangle\!\rangle = \frac{1}{\alpha^2 - \beta^2}\int_{\Gamma} (\phi\nabla\psi\cdot\boldsymbol{n} - \psi\nabla\phi\cdot\boldsymbol{n})\mathrm{d}\ell,$$

for arbitrary boundary conditions on ϕ and ψ

What if $\alpha = \beta$ and $\phi = \psi$? Something similar.

Closed form integrals of 2D eigenmodes

Prototype example of *Generalised Pridmore-Brown* : Helmholtz equation

$$
\begin{aligned}
\phi\left(\nabla^2\psi + \beta^2\psi\right) &= 0\\
\psi\left(\nabla^2\phi + \alpha^2\phi\right) &= 0
\end{aligned}
$$

on arbitrarily shaped cross-section $\mathcal{A}$
Subtract and integrate over $\mathcal{A}$

$$(\alpha^2-\beta^2)\iint_{\mathcal{A}}\phi\psi\,\mathrm{d}S \;\overset{\text{GAUSS}}{=}\; \iint_{\mathcal{A}}\nabla\cdot(\phi\nabla\psi-\psi\nabla\phi)\,\mathrm{d}S$$

2D inner-product for Helmholtz eigenfunctions

$$\langle\!\langle\phi,\psi\rangle\!\rangle = \frac{1}{\alpha^2-\beta^2}\int_{\Gamma}(\phi\nabla\psi\cdot\boldsymbol{n}-\psi\nabla\phi\cdot\boldsymbol{n})\mathrm{d}\ell,$$

for arbitrary boundary conditions on ϕ and ψ

What if $\alpha=\beta$ and $\phi=\psi$? Something similar.

Closed form integrals of 2D eigenmodes

Prototype example of *Generalised Pridmore-Brown* : Helmholtz equation

$$\phi\left(\nabla^2\psi + \beta^2\psi\right) = 0$$
$$\psi\left(\nabla^2\phi + \alpha^2\phi\right) = 0$$

on arbitrarily shaped cross-section $\mathcal{A}$
Subtract and integrate over $\mathcal{A}$

$$(\alpha^2 - \beta^2)\iint_{\mathcal{A}} \phi\psi \,\mathrm{d}S = \overset{\text{GAUSS}}{\overset{\downarrow}{\iint_{\mathcal{A}}}} \nabla\cdot(\phi\nabla\psi - \psi\nabla\phi)\,\mathrm{d}S$$

2D inner-product for Helmholtz eigenfunctions

$$\langle\!\langle \phi, \psi \rangle\!\rangle = \frac{1}{\alpha^2 - \beta^2}\int_\Gamma (\phi\nabla\psi\cdot\boldsymbol{n} - \psi\nabla\phi\cdot\boldsymbol{n})\mathrm{d}\ell,$$

for arbitrary boundary conditions on ϕ and ψ

What if $\alpha = \beta$ and $\phi = \psi$? Something similar.

Closed form integrals of 2D eigenmodes

Prototype example of *Generalised Pridmore-Brown* : Helmholtz equation

$$\phi\left(\nabla^2\psi + \beta^2\psi\right) = 0$$
$$\psi\left(\nabla^2\phi + \alpha^2\phi\right) = 0$$

on arbitrarily shaped cross-section $\mathcal{A}$
Subtract and integrate over $\mathcal{A}$

$$(\alpha^2 - \beta^2)\iint_{\mathcal{A}} \phi\psi \,\mathrm{d}S = \overset{\text{GAUSS}}{\overset{\downarrow}{\int_\Gamma}} (\phi\nabla\psi\cdot\boldsymbol{n} - \psi\nabla\phi\cdot\boldsymbol{n})\,\mathrm{d}\ell$$

2D inner-product for Helmholtz eigenfunctions

$$\langle\langle\phi,\psi\rangle\rangle = \frac{1}{\alpha^2-\beta^2}\int_\Gamma(\phi\nabla\psi\cdot\boldsymbol{n} - \psi\nabla\phi\cdot\boldsymbol{n})\mathrm{d}\ell,$$

for arbitrary boundary conditions on ϕ and ψ

What if $\alpha = \beta$ and $\phi = \psi$? Something similar.

Closed form integrals of 2D eigenmodes

Prototype example of *Generalised Pridmore-Brown* : Helmholtz equation

$$\phi\left(\nabla^2\psi + \beta^2\psi\right) = 0$$
$$\psi\left(\nabla^2\phi + \alpha^2\phi\right) = 0$$

on arbitrarily shaped cross-section $\mathcal{A}$
Subtract and integrate over $\mathcal{A}$

$$(\alpha^2 - \beta^2)\iint_{\mathcal{A}} \phi\psi \,\mathrm{d}S = \overset{\substack{\text{GAUSS}\\ \downarrow}}{\int_{\Gamma}} (\phi\nabla\psi\cdot\boldsymbol{n} - \psi\nabla\phi\cdot\boldsymbol{n})\,\mathrm{d}\ell$$

2D inner-product for Helmholtz eigenfunctions

$$\langle\!\langle \phi, \psi \rangle\!\rangle = \frac{1}{\alpha^2 - \beta^2}\int_{\Gamma}(\phi\nabla\psi\cdot\boldsymbol{n} - \psi\nabla\phi\cdot\boldsymbol{n})\mathrm{d}\ell,$$

for arbitrary boundary conditions on ϕ and ψ

What if $\alpha = \beta$ and $\phi = \psi$? Something similar.

Closed form integrals of 2D eigenmodes

Prototype example of *Generalised Pridmore-Brown* : Helmholtz equation

$$\phi\left(\nabla^2\psi+\beta^2\psi\right)=0$$
$$\psi\left(\nabla^2\phi+\alpha^2\phi\right)=0$$

on arbitrarily shaped cross-section $\mathcal{A}$
Subtract and integrate over $\mathcal{A}$

GAUSS

$$(\alpha^2-\beta^2)\iint_{\mathcal{A}}\phi\psi\,\mathrm{d}S\;=\;\int_{\Gamma}(\phi\boldsymbol{\nabla}\psi\cdot\boldsymbol{n}-\psi\boldsymbol{\nabla}\phi\cdot\boldsymbol{n})\,\mathrm{d}\ell$$

2D inner-product for Helmholtz eigenfunctions

$$\langle\!\langle\phi,\psi\rangle\!\rangle=\frac{1}{\alpha^2-\beta^2}\int_{\Gamma}(\phi\boldsymbol{\nabla}\psi\cdot\boldsymbol{n}-\psi\boldsymbol{\nabla}\phi\cdot\boldsymbol{n})\mathrm{d}\ell,$$

for arbitrary boundary conditions on ϕ and ψ

What if $\alpha=\beta$ and $\phi=\psi$? Something similar.

Closed form integrals of 1D eigenmodes

- Circular duct: Helmholtz equation → Bessel equation
- Substitute into 2D inner-product:

$$\phi = J_m(\alpha r)\, \mathrm{e}^{\mathrm{i}m\theta},\ \psi = J_m(\beta r)\, \mathrm{e}^{-\mathrm{i}m\theta}$$

1D inner-product of Bessel functions

$$\langle J_m(\alpha r), J_m(\beta r)\rangle = \int_0^1 J_m(\alpha r) J_m(\beta r)\, r\, \mathrm{d}r$$
$$= \frac{1}{\alpha^2 - \beta^2}\left[\beta J_m(\alpha) J_m'(\beta) - \alpha J_m'(\alpha) J_m(\beta)\right]$$

If $\alpha = \beta$: something similar.

Closed form integrals of 1D eigenmodes

- Circular duct: Helmholtz equation → Bessel equation
- Substitute into 2D inner-product:

$$\phi = J_m(\alpha r)\,\mathrm{e}^{\mathrm{i}m\theta},\ \psi = J_m(\beta r)\,\mathrm{e}^{-\mathrm{i}m\theta}$$

1D inner-product of Bessel functions

$$\begin{aligned}\langle J_m(\alpha r),\, J_m(\beta r)\rangle &= \int_0^1 J_m(\alpha r)\,J_m(\beta r)\,r\,\mathrm{d}r \\ &= \frac{1}{\alpha^2-\beta^2}\left[\beta\,J_m(\alpha)\,J_m'(\beta) - \alpha\,J_m'(\alpha)\,J_m(\beta)\right]\end{aligned}$$

If $\alpha = \beta$: something similar.

Closed form integrals of 1D eigenmodes

- Circular duct: Helmholtz equation → Bessel equation
- Substitute into 2D inner-product:

$$\phi = J_m(\alpha r)\,\mathrm{e}^{\mathrm{i}m\theta},\ \psi = J_m(\beta r)\,\mathrm{e}^{-\mathrm{i}m\theta}$$

1D inner-product of Bessel functions

$$\begin{aligned}\langle J_m(\alpha r),\, J_m(\beta r)\rangle &= \int_0^1 J_m(\alpha r)\, J_m(\beta r)\, r\,\mathrm{d}r \\ &= \frac{1}{\alpha^2 - \beta^2}\left[\beta\, J_m(\alpha)\, J_m'(\beta) - \alpha\, J_m'(\alpha)\, J_m(\beta)\right]\end{aligned}$$

If $\alpha = \beta$: something similar.

Closed form integrals for Generalised P-B modes

By analogous manipulations ...

- Define vector of shape functions $\boldsymbol{F}(y, z) = \left[P, U, V, W\right]$
- P solution of Generalised PB equation, U, V, W follow from P

Similarly to 2D Helmholtz example, it can be found:

Closed form integral of parallel flow modes

$$\langle\langle \boldsymbol{F}, \tilde{\boldsymbol{F}} \rangle\rangle = \iint_{\mathcal{A}} \frac{1}{\tilde{\Omega}} \left[\left(\frac{u_0}{\rho_0 c_0^2} + \frac{\tilde{k}}{\rho_0 \tilde{\Omega}} \right) \tilde{P} P + \frac{\omega}{\tilde{\Omega}} \tilde{P} U - \rho_0 u_0 (\tilde{V} V + \tilde{W} W) \right] \mathrm{d}S$$
$$= \frac{\mathrm{i}}{k - \tilde{k}} \int_{\Gamma} \frac{\tilde{P}(V n_y + W n_z) - (\tilde{V} n_y + \tilde{W} n_z) P}{\tilde{\Omega}} \, \mathrm{d}\ell,$$

Something similar for $k = \tilde{k}$.

By analogous manipulations ...

- Define vector of shape functions $\boldsymbol{F}(y,z) = \left[P, U, V, W\right]$
- P solution of Generalised PB equation, U, V, W follow from P

Similarly to 2D Helmholtz example, it can be found:

Closed form integral of parallel flow modes

$$\langle\langle \boldsymbol{F}, \tilde{\boldsymbol{F}} \rangle\rangle = \iint_{\mathcal{A}} \frac{1}{\tilde{\Omega}} \left[\left(\frac{u_0}{\rho_0 c_0^2} + \frac{\tilde{k}}{\rho_0 \tilde{\Omega}} \right) \tilde{P} P + \frac{\omega}{\tilde{\Omega}} \tilde{P} U - \rho_0 u_0 (\tilde{V} V + \tilde{W} W) \right] \mathrm{d}S$$

$$= \frac{\mathrm{i}}{k - \tilde{k}} \int_{\Gamma} \frac{\tilde{P}(V n_y + W n_z) - (\tilde{V} n_y + \tilde{W} n_z) P}{\tilde{\Omega}} \, \mathrm{d}\ell,$$

Something similar for $k = \tilde{k}$.

Closed form integrals for Generalised P-B modes

By analogous manipulations ...

- Define vector of shape functions $\boldsymbol{F}(y,z) = \left[P, U, V, W\right]$
- P solution of Generalised PB equation, U, V, W follow from P

Similarly to 2D Helmholtz example, it can be found:

Closed form integral of parallel flow modes

$$\langle\langle \boldsymbol{F}, \tilde{\boldsymbol{F}} \rangle\rangle =$$

$$\iint_{\mathcal{A}} \frac{1}{\tilde{\Omega}} \left[\left(\frac{u_0}{\rho_0 c_0^2} + \frac{\tilde{k}}{\rho_0 \tilde{\Omega}} \right) \tilde{P} P + \frac{\omega}{\tilde{\Omega}} \tilde{P} U - \rho_0 u_0 (\tilde{V} V + \tilde{W} W) \right] \mathrm{d}S$$

$$= \frac{\mathrm{i}}{k - \tilde{k}} \int_{\Gamma} \frac{\tilde{P}(V n_y + W n_z) - (\tilde{V} n_y + \tilde{W} n_z) P}{\tilde{\Omega}} \, \mathrm{d}\ell,$$

Something similar for $k = \tilde{k}$.

Closed form integrals for Generalised P-B modes

By analogous manipulations . . .

- Define vector of shape functions $\boldsymbol{F}(y,z) = \big[P, U, V, W\big]$
- P solution of Generalised PB equation, U, V, W follow from P

Similarly to 2D Helmholtz example, it can be found:

Closed form integral of parallel flow modes

$$\langle\!\langle \boldsymbol{F}, \tilde{\boldsymbol{F}} \rangle\!\rangle =$$

$$\iint_{\mathcal{A}} \frac{1}{\tilde{\Omega}} \left[\left(\frac{u_0}{\rho_0 c_0^2} + \frac{\tilde{k}}{\rho_0 \tilde{\Omega}} \right) \tilde{P} P + \frac{\omega}{\tilde{\Omega}} \tilde{P} U - \rho_0 u_0 (\tilde{V} V + \tilde{W} W) \right] \mathrm{d}S$$

$$= \frac{\mathrm{i}}{k - \tilde{k}} \int_{\Gamma} \frac{\tilde{P}(V n_y + W n_z) - (\tilde{V} n_y + \tilde{W} n_z) P}{\tilde{\Omega}} \, \mathrm{d}\ell,$$

Something similar for $k = \tilde{k}$.

Substitute for circular symmetric geometry…

modes of the form $\boldsymbol{F}(r)\,\mathrm{e}^{\pm \mathrm{i} m\theta}$

$$\boldsymbol{F}(r) = [P(r), U(r), V(r), W(r)]$$

- P solution of the radial Pridmore-Brown equation
- U, V, W follow from P

Exact integrals of radial Pridmore-Brown modes

$$\langle \boldsymbol{F}, \tilde{\boldsymbol{F}} \rangle = \int_0^1 \frac{1}{\tilde{\Omega}} \left[\left(\frac{u_0}{\rho_0 c_0^2} + \frac{\tilde{k}}{\rho_0 \tilde{\Omega}} \right) P\tilde{P} + \frac{\omega}{\tilde{\Omega}} U\tilde{P} - \rho_0 u_0 (V\tilde{V} + W\tilde{W}) \right] r\,\mathrm{d}r$$

$$= \frac{\mathrm{i}}{k - \tilde{k}} \left[\frac{\tilde{P}V - \tilde{V}P}{\tilde{\Omega}} \right]_{r=1}$$

Weighted products of Pridmore-Brown eigenfunctions.
Something similar for $k = \tilde{k}$.

Closed form integrals for radial Pridmore-Brown modes

Substitute for circular symmetric geometry. . .
modes of the form $\boldsymbol{F}(r)\,\mathrm{e}^{\pm\mathrm{i}m\theta}$

$$\boldsymbol{F}(r) = [P(r), U(r), V(r), W(r)]$$

- P solution of the radial Pridmore-Brown equation
- U, V, W follow from P

Exact integrals of radial Pridmore-Brown modes

$$\langle \boldsymbol{F}, \tilde{\boldsymbol{F}} \rangle =$$

$$\int_0^1 \frac{1}{\tilde{\Omega}} \left[\left(\frac{u_0}{\rho_0 c_0^2} + \frac{\tilde{k}}{\rho_0 \tilde{\Omega}} \right) P \tilde{P} + \frac{\omega}{\tilde{\Omega}} U \tilde{P} - \rho_0 u_0 (V \tilde{V} + W \tilde{W}) \right] r \, \mathrm{d}r$$

$$= \frac{\mathrm{i}}{k - \tilde{k}} \left[\frac{\tilde{P} V - \tilde{V} P}{\tilde{\Omega}} \right]_{r=1}$$

Weighted products of Pridmore-Brown eigenfunctions.
Something similar for $k = \tilde{k}$.

Closed form integrals for radial Pridmore-Brown modes

Substitute for circular symmetric geometry…

modes of the form $\boldsymbol{F}(r)\,\mathrm{e}^{\pm \mathrm{i} m\theta}$

$$\boldsymbol{F}(r) = [P(r), U(r), V(r), W(r)]$$

- P solution of the radial Pridmore-Brown equation
- U, V, W follow from P

Exact integrals of radial Pridmore-Brown modes

$$\langle \boldsymbol{F}, \tilde{\boldsymbol{F}} \rangle =$$

$$\int_0^1 \frac{1}{\tilde{\Omega}} \left[\left(\frac{u_0}{\rho_0 c_0^2} + \frac{\tilde{k}}{\rho_0 \tilde{\Omega}} \right) P \tilde{P} + \frac{\omega}{\tilde{\Omega}} U \tilde{P} - \rho_0 u_0 (V \tilde{V} + W \tilde{W}) \right] r \,\mathrm{d}r$$

$$= \frac{\mathrm{i}}{k - \tilde{k}} \left[\frac{\tilde{P} V - \tilde{V} P}{\tilde{\Omega}} \right]_{r=1}$$

Weighted products of Pridmore-Brown eigenfunctions.
Something similar for $k = \tilde{k}$.

Closed form integrals for radial Pridmore-Brown modes

Substitute for circular symmetric geometry…
modes of the form $\boldsymbol{F}(r)\, \mathrm{e}^{\pm \mathrm{i} m\theta}$

$$\boldsymbol{F}(r) = [P(r), U(r), V(r), W(r)]$$

- P solution of the radial Pridmore-Brown equation
- U, V, W follow from P

Exact integrals of radial Pridmore-Brown modes

$$\langle \boldsymbol{F}, \tilde{\boldsymbol{F}} \rangle = \int_0^1 \frac{1}{\tilde{\Omega}} \left[\left(\frac{u_0}{\rho_0 c_0^2} + \frac{\tilde{k}}{\rho_0 \tilde{\Omega}} \right) P \tilde{P} + \frac{\omega}{\tilde{\Omega}} U \tilde{P} - \rho_0 u_0 (V \tilde{V} + W \tilde{W}) \right] r \, \mathrm{d}r = \frac{\mathrm{i}}{k - \tilde{k}} \left[\frac{\tilde{P} V - \tilde{V} P}{\tilde{\Omega}} \right]_{r=1}$$

Weighted products of Pridmore-Brown eigenfunctions.
Something similar for $k = \tilde{k}$.

New mode-matching

Classic mode-matching (CMM)

$$\sum_{\mu=1}^{\mu_l} b^+_{l,\mu}(P^+_{l,\mu}, \Psi_\nu) + a^-_{l,\mu}(P^-_{l,\mu}, \Psi_\nu)$$
$$= \sum_{\mu=1}^{\mu_{l+1}} a^+_{l+1,\mu}(P^+_{l+1,\mu}, \Psi_\nu) + b^-_{l+1,\mu}(P^-_{l+1,\mu}, \Psi_\nu)$$

(same for velocity) with test functions (for example)

$$\Psi_\nu = J_m(\alpha_\nu r)$$

Quadrature required for (P_μ, Ψ_ν) terms

New mode-matching

Classic mode-matching (CMM)

$$\sum_{\mu=1}^{\mu_l} b^+_{l,\mu}(P^+_{l,\mu},\Psi_\nu) + a^-_{l,\mu}(P^-_{l,\mu},\Psi_\nu)$$

$$= \sum_{\mu=1}^{\mu_{l+1}} a^+_{l+1,\mu}(P^+_{l+1,\mu},\Psi_\nu) + b^-_{l+1,\mu}(P^-_{l+1,\mu},\Psi_\nu)$$

(same for velocity) with test functions (for example)

$$\Psi_\nu = J_m(\alpha_\nu r)$$

Quadrature required for (P_μ, Ψ_ν) terms

New mode-matching

New* (NMM) mode-matching

$$\sum_{\mu=1}^{\mu_l} b^{+}_{l,\mu}\langle \boldsymbol{F}^{+}_{l,\mu}, \boldsymbol{\Psi}_\nu\rangle + a^{-}_{l,\mu}\langle \boldsymbol{F}^{-}_{l,\mu}, \boldsymbol{\Psi}_\nu\rangle$$
$$= \sum_{\mu=1}^{\mu_{l+1}} a^{+}_{l+1,\mu}\langle \boldsymbol{F}^{+}_{l+1,\mu}, \boldsymbol{\Psi}_\nu\rangle + b^{-}_{l+1,\mu}\langle \boldsymbol{F}^{-}_{l+1,\mu}, \boldsymbol{\Psi}_\nu\rangle$$

but now as test functions the same modes:

$$\boldsymbol{\Psi}_\nu = \boldsymbol{F}_{l,\nu}$$

No extra calculations *and* $\langle \boldsymbol{F}_\mu, \boldsymbol{\Psi}_\nu\rangle$ in closed form

*Technically not an inner-product, except for no flow or uniform flow.

New mode-matching

New* (NMM) mode-matching

$$\sum_{\mu=1}^{\mu_l} b^+_{l,\mu}\langle \boldsymbol{F}^+_{l,\mu}, \boldsymbol{\Psi}_\nu\rangle + a^-_{l,\mu}\langle \boldsymbol{F}^-_{l,\mu}, \boldsymbol{\Psi}_\nu\rangle$$

$$= \sum_{\mu=1}^{\mu_{l+1}} a^+_{l+1,\mu}\langle \boldsymbol{F}^+_{l+1,\mu}, \boldsymbol{\Psi}_\nu\rangle + b^-_{l+1,\mu}\langle \boldsymbol{F}^-_{l+1,\mu}, \boldsymbol{\Psi}_\nu\rangle$$

but now as test functions the same modes:

$$\boldsymbol{\Psi}_\nu = \boldsymbol{F}_{l,\nu}$$

No extra calculations *and* $\langle \boldsymbol{F}_\mu, \boldsymbol{\Psi}_\nu\rangle$ in closed form

*Technically not an inner-product, except for no flow or uniform flow.

New mode-matching

New* (NMM) mode-matching

$$\sum_{\mu=1}^{\mu_l} b^+_{l,\mu} \langle \boldsymbol{F}^+_{l,\mu}, \boldsymbol{\Psi}_\nu \rangle + a^-_{l,\mu} \langle \boldsymbol{F}^-_{l,\mu}, \boldsymbol{\Psi}_\nu \rangle$$

$$= \sum_{\mu=1}^{\mu_{l+1}} a^+_{l+1,\mu} \langle \boldsymbol{F}^+_{l+1,\mu}, \boldsymbol{\Psi}_\nu \rangle + b^-_{l+1,\mu} \langle \boldsymbol{F}^-_{l+1,\mu}, \boldsymbol{\Psi}_\nu \rangle$$

but now as test functions the same modes:

$$\boldsymbol{\Psi}_\nu = \boldsymbol{F}_{l,\nu}$$

No extra calculations *and* $\langle \boldsymbol{F}_\mu, \boldsymbol{\Psi}_\nu \rangle$ in closed form

*Technically not an inner-product, except for no flow or uniform flow.

Comparing CMM and NMM

Test configurations

- Length: 6.66
- Radius: 1
- hard wall – soft wall, interface at x = 3.33
- $\mu^{\max}$ = 50 modes in both directions

Configuration	I	II	III
Helmholtz & m	$\omega = 13.86, m = 5$	$\omega = 8.86, m = 5$	$\omega = 15, m = 5$
Temperature	$T_0 = 1$	$T_0 = 1$	$T_0 = 2\log(2)(1-\frac{r^2}{2})$
Mean flow	$u_0 = 0.5 \cdot (1 - r^2)$	$u_0 = 0.3 \cdot \frac{4}{3}(1-\frac{r^2}{2})$	$u_0 = 0.3 \cdot \tanh(10(1-r))$
Impedance	$Z = 1 - \mathrm{i}$	$Z = 1 + \mathrm{i}$	$Z = 1 - \mathrm{i}$
Incident mode	$\mu = 1$	$\mu = 1$	$\mu = 2$

Numerical results — Conf I: no-slip flow, uniform temp

Snap shot of pressure

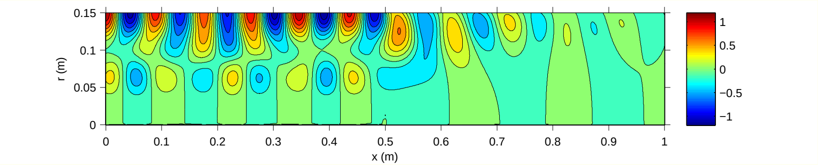

(a) Classical mode-matching.

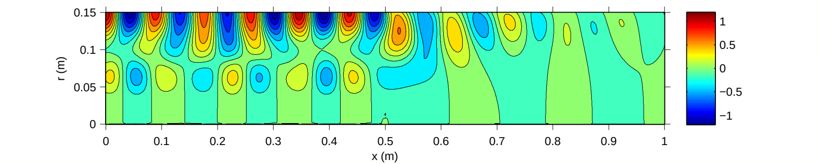

(b) New mode-matching.

Perfect match between NMM and CMM results

Numerical results — Conf I: no-slip flow, uniform temp

Pressure at $r = \{0.233, 0.5, 1\}$ m.

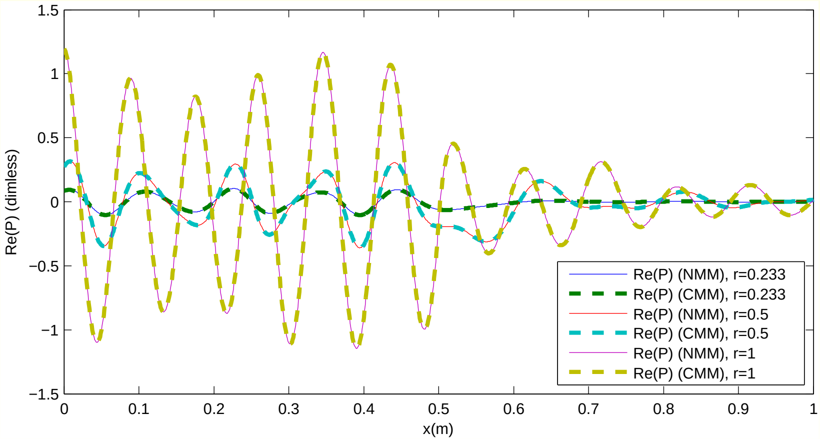

Perfect match between NMM and CMM results

Similar for axial and radial velocities

Pressure at $r = \{0.233, 0.5, 1\}$ m.

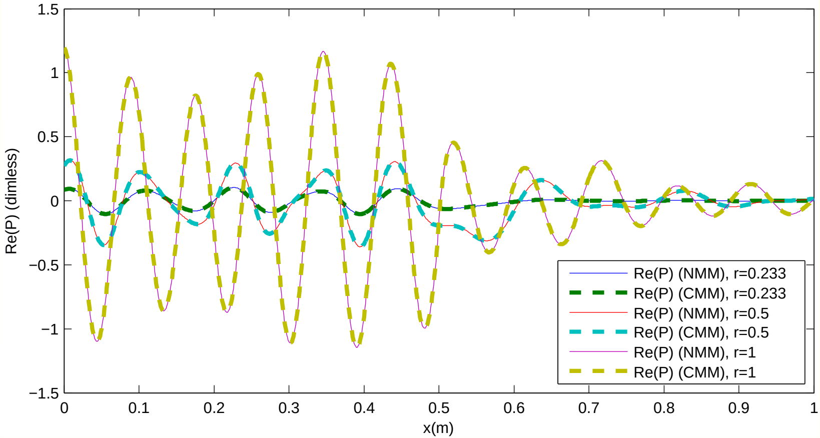

Perfect match between NMM and CMM results

Similar for axial and radial velocities

Numerical results — Energy balance

Energy balance (Myers' Energy Corollary) vs $\mu^{\max}$ for conf. I

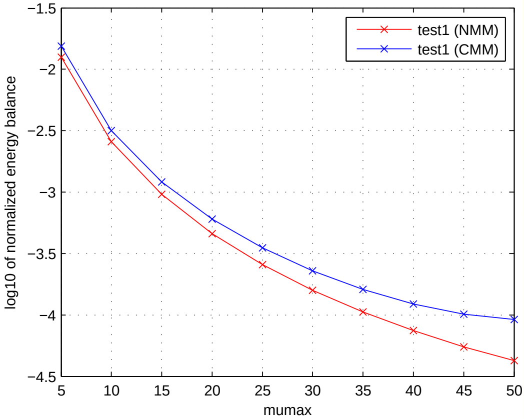

Energy balance better with more μ-modes.
NMM performs better than CMM! Why?

Energy balance (Myers' Energy Corollary) vs $\mu^{\max}$ for conf. I

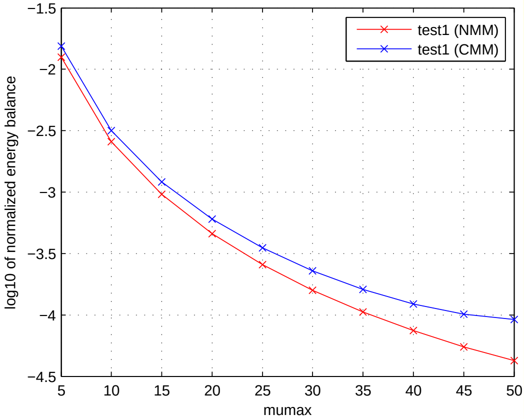

Energy balance better with more μ-modes.

NMM performs better than CMM! Why?

Energy balance (Myers' Energy Corollary) vs $\mu^{\max}$ for conf. I

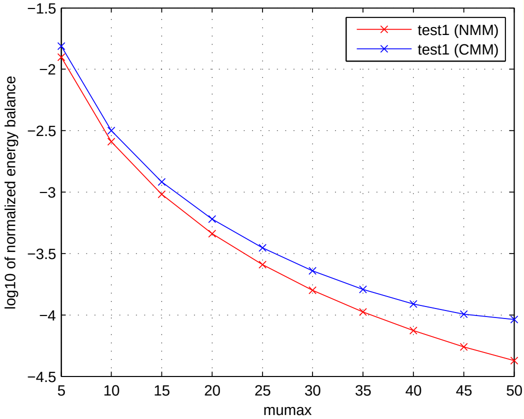

Energy balance better with more μ-modes.
NMM performs better than CMM! Why?

Energy balance (Myers' Energy Corollary) vs $\mu^{\max}$ for conf. I

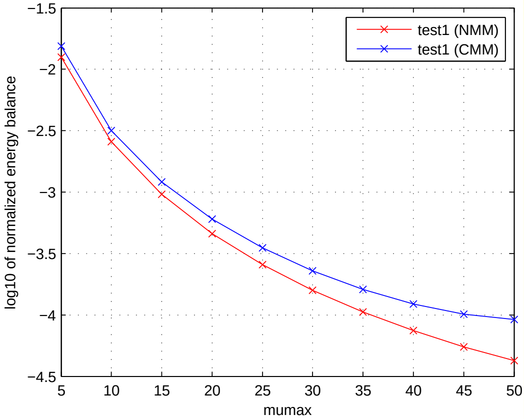

Energy balance better with more μ-modes.
NMM performs better than CMM! Why?

Edge Condition (a posteriori check)

It is reasonable to assume that for some $q < 0$ the amplitudes

$$A_\mu = O(\mu^q) \quad \text{for} \quad \mu \to \infty$$

so $\log |A_\mu| = q \log \mu + O(1)$. Then

$$q_\mu = \frac{\log |A_\mu|}{\log \mu} \to q \quad \text{for} \quad \mu \to \infty$$

At the interface, at the wall (*edge*): boundary cond. discontinuous. Field may be singular, but Power Flux must vanish at edge.

It can be shown that:

$$q < -1 \Rightarrow \text{uniform convergence of modal series}$$
$$\Rightarrow \text{edge condition satisfied}$$

Edge Condition (a posteriori check)

It is reasonable to assume that for some $q < 0$ the amplitudes

$$A_\mu = O(\mu^q) \quad \text{for} \quad \mu \to \infty$$

so $\log|A_\mu| = q \log\mu + O(1)$. Then

$$q_\mu = \frac{\log|A_\mu|}{\log\mu} \to q \quad \text{for} \quad \mu \to \infty$$

At the interface, at the wall (*edge*): boundary cond. discontinuous.
Field may be singular, but Power Flux must vanish at edge.

It can be shown that:

$$q < -1 \Rightarrow \text{uniform convergence of modal series}$$
$$\Rightarrow \text{edge condition satisfied}$$

Edge Condition (a posteriori check)

It is reasonable to assume that for some $q < 0$ the amplitudes

$$A_\mu = O(\mu^q) \quad \text{for} \quad \mu \to \infty$$

so $\log|A_\mu| = q \log \mu + O(1)$. Then

$$q_\mu = \frac{\log|A_\mu|}{\log \mu} \to q \quad \text{for} \quad \mu \to \infty$$

At the interface, at the wall (*edge*): boundary cond. discontinuous.
Field may be singular, but Power Flux must vanish at edge.

It can be shown that:

$$q < -1 \Rightarrow \text{uniform convergence of modal series}$$
$$\Rightarrow \text{edge condition satisfied}$$

Numerical results — Convergence of modal amplitudes

Edge Condition (a posteriori check)

It is reasonable to assume that for some $q < 0$ the amplitudes

$$A_\mu = O(\mu^q) \quad \text{for} \quad \mu \to \infty$$

so $\log |A_\mu| = q \log \mu + O(1)$. Then

$$q_\mu = \frac{\log |A_\mu|}{\log \mu} \to q \quad \text{for} \quad \mu \to \infty$$

At the interface, at the wall (*edge*): boundary cond. discontinuous.
Field may be singular, but Power Flux must vanish at edge.

It can be shown that:

$$q < -1 \Rightarrow \text{uniform convergence of modal series}$$
$$\Rightarrow \text{edge condition satisfied}$$

Edge Condition (a posteriori check)

It is reasonable to assume that for some $q < 0$ the amplitudes

$$A_\mu = O(\mu^q) \quad \text{for} \quad \mu \to \infty$$

so $\log|A_\mu| = q \log \mu + O(1)$. Then

$$q_\mu = \frac{\log|A_\mu|}{\log \mu} \to q \quad \text{for} \quad \mu \to \infty$$

At the interface, at the wall (*edge*): boundary cond. discontinuous.
Field may be singular, but Power Flux must vanish at edge.

It can be shown that:

$$\begin{aligned} q < -1 &\Rightarrow \text{uniform convergence of modal series} \\ &\Rightarrow \text{edge condition satisfied} \end{aligned}$$

Numerical results — Convergence of modal amplitudes

Do we have $q < -1$ for numerical solutions?

- $q \approx -2 \Rightarrow$ edge condition satisfied ✓
- Convergence of q_μ reveals inaccuracies of CMM amplitudes:
  - NMM amplitudes are smoother than CMM as $\mu \sim \mu^{\max}$, because no quadrature inaccuracies for NMM.
  - Explains energy behaviour.

Do we have $q < -1$ for numerical solutions?

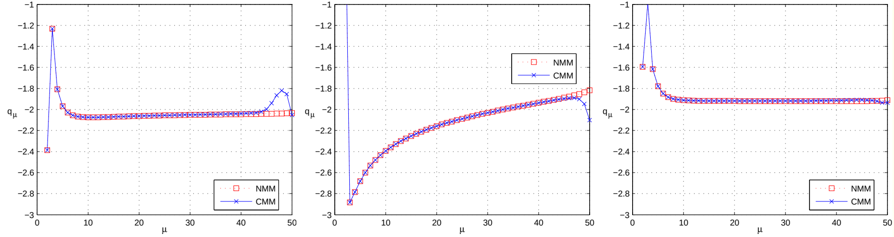

Convergence of amplitudes (NMM and CMM), for conf. I, II and III

- $q \approx -2 \Rightarrow$ edge condition satisfied ✓
- Convergence of q_μ reveals inaccuracies of CMM amplitudes:
  - NMM amplitudes are smoother than CMM as $\mu \sim \mu^{\max}$, because no quadrature inaccuracies for NMM.
  - Explains energy behaviour.

Do we have $q < -1$ for numerical solutions?

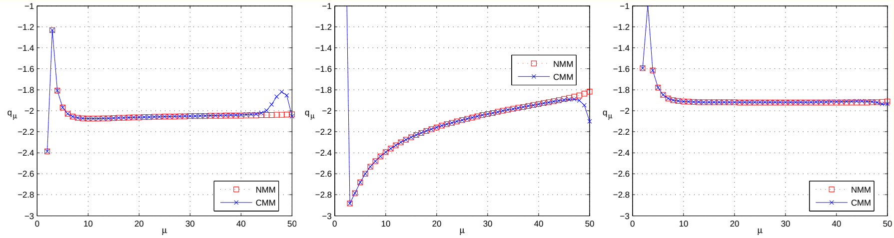

Convergence of amplitudes (NMM and CMM), for conf. I, II and III

- $q \approx -2 \Rightarrow$ edge condition satisfied ✓
- Convergence of q_μ reveals inaccuracies of CMM amplitudes:
  - NMM amplitudes are smoother than CMM as $\mu \sim \mu^{\max}$, because no quadrature inaccuracies for NMM.
  - Explains energy behaviour.

Do we have $q < -1$ for numerical solutions?

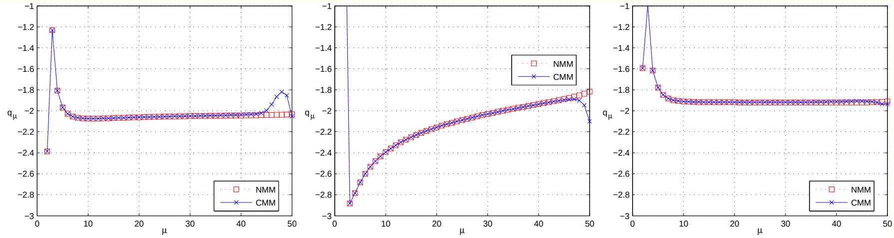

Convergence of amplitudes (NMM and CMM), for conf. I, II and III

- $q \approx -2 \Rightarrow$ edge condition satisfied ✓
- Convergence of q_μ reveals inaccuracies of CMM amplitudes:
  - NMM amplitudes are smoother than CMM as $\mu \sim \mu^{\max}$, because no quadrature inaccuracies for NMM.
  - Explains energy behaviour.

Do we have $q < -1$ for numerical solutions?

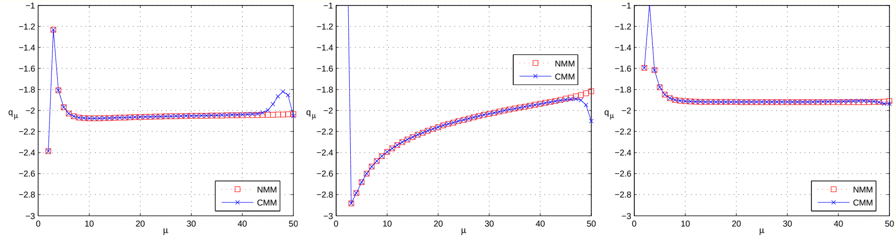

Convergence of amplitudes (NMM and CMM), for conf. I, II and III

- $q \approx -2 \Rightarrow$ edge condition satisfied ✓
- Convergence of q_μ reveals inaccuracies of CMM amplitudes:
  - $*$ NMM amplitudes are smoother than CMM as $\mu \sim \mu^{\max}$, because no quadrature inaccuracies for NMM.
  - $*$ Explains energy behaviour.

Do we have $q < -1$ for numerical solutions?

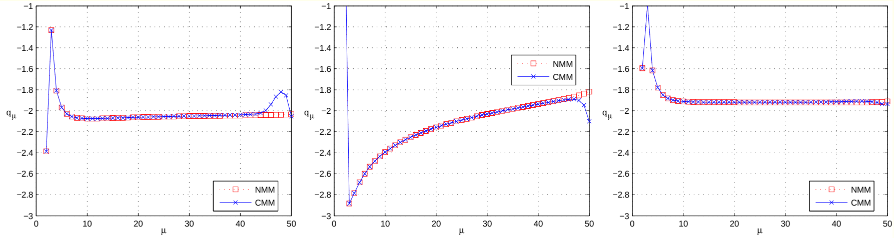

Convergence of amplitudes (NMM and CMM), for conf. I, II and III

- $q \approx -2 \Rightarrow$ edge condition satisfied ✓
- Convergence of q_μ reveals inaccuracies of CMM amplitudes:
  - ∗ NMM amplitudes are smoother than CMM as $\mu \sim \mu^{\max}$, because no quadrature inaccuracies for NMM.
  - ∗ Explains energy behaviour.

Interim conclusions

Classic mode-matching (CMM):

- Uniform flow & temp:
  - Mode shapes are Bessel functions
  - Inner products are available in closed form
- Parallel (non-uniform) flow & temp:
  - Mode shapes are Pridmore-Brown solutions (determined numerically)
  - Inner products require numerical quadrature
    $\rightarrow$ expensive & less accurate

New mode-matching (NMM):

- Parallel (non-uniform) flow & temp:
  - Mode shapes are Pridmore-Brown solutions (determined numerically)
  - Closed form expressions for "inner-products" cheaper
  - Solutions in very good agreement with CMM
  - NMM amplitudes more accurate

Interim conclusions

Classic mode-matching (CMM):

- Uniform flow & temp:
  - Mode shapes are Bessel functions
  - Inner products are available in closed form
- Parallel (non-uniform) flow & temp:
  - Mode shapes are Pridmore-Brown solutions (determined numerically)
  - Inner products require numerical quadrature
    $\rightarrow$ expensive & less accurate

New mode-matching (NMM):

- Parallel (non-uniform) flow & temp:
  - Mode shapes are Pridmore-Brown solutions (determined numerically)
  - Closed form expressions for “inner-products” cheaper
  - Solutions in very good agreement with CMM
  - NMM amplitudes more accurate

Interim conclusions

Classic mode-matching (CMM):

- Uniform flow & temp:
  - Mode shapes are Bessel functions
  - Inner products are available in closed form
- Parallel (non-uniform) flow & temp:
  - Mode shapes are Pridmore-Brown solutions (determined numerically)
  - Inner products require numerical quadrature
    $\rightarrow$ expensive & less accurate

New mode-matching (NMM):

- Parallel (non-uniform) flow & temp:
  - Mode shapes are Pridmore-Brown solutions (determined numerically)
  - Closed form expressions for "inner-products" cheaper
  - Solutions in very good agreement with CMM
  - NMM amplitudes more accurate

Interim conclusions

Classic mode-matching (CMM):

- Uniform flow & temp:
  - Mode shapes are Bessel functions
  - Inner products are available in closed form
- Parallel (non-uniform) flow & temp:
  - Mode shapes are Pridmore-Brown solutions (determined numerically)
  - Inner products require numerical quadrature
    $\rightarrow$ expensive & less accurate

New mode-matching (NMM):

- Parallel (non-uniform) flow & temp:
  - Mode shapes are Pridmore-Brown solutions (determined numerically)
  - Closed form expressions for “inner-products” cheaper
  - Solutions in very good agreement with CMM
  - NMM amplitudes more accurate

Interim conclusions

Classic mode-matching (CMM):

- Uniform flow & temp:
  - Mode shapes are Bessel functions
  - Inner products are available in closed form
- Parallel (non-uniform) flow & temp:
  - Mode shapes are Pridmore-Brown solutions (determined numerically)
  - Inner products require numerical quadrature
    $\rightarrow$ expensive & less accurate

New mode-matching (NMM):

- Parallel (non-uniform) flow & temp:
  - Mode shapes are Pridmore-Brown solutions (determined numerically)
  - Closed form expressions for "inner-products" cheaper
  - Solutions in very good agreement with CMM
  - NMM amplitudes more accurate

Epilogue

- The success of NMM is, in a way, too good. At least far better than expected, because the “inner-product” is not a proper inner-product (unless $u_0 = 0$ or uniform) and we can’t be sure that it is able to single out each modal contribution.
- Nevertheless, from the success we can only conclude that it must be “almost” an inner-product. The modes are all “seen” and distinguished.
- The “inner-product” is not exactly an inner-product because the set of discrete modes is not complete, i.e. not sufficient to construct *any* possible solution. There is a “continuous” spectrum at the locus of $\omega - ku_0(r) = 0$. From the energy result we can (again) conclude that this part is very small.
- A fine task in functional analysis remains . . .

Epilogue

- The success of NMM is, in a way, too good. At least far better than expected, because the "inner-product" is not a proper inner-product (unless $u_0 = 0$ or uniform) and we can't be sure that it is able to single out each modal contribution.
- Nevertheless, from the success we can only conclude that it must be "almost" an inner-product. The modes are all "seen" and distinguished.
- The "inner-product" is not exactly an inner-product because the set of discrete modes is not complete, i.e. not sufficient to construct *any* possible solution. There is a "continuous" spectrum at the locus of $\omega - ku_0(r) = 0$. From the energy result we can (again) conclude that this part is very small.
- A fine task in functional analysis remains ...

Epilogue

- The success of NMM is, in a way, too good. At least far better than expected, because the “inner-product” is not a proper inner-product (unless $u_0 = 0$ or uniform) and we can’t be sure that it is able to single out each modal contribution.
- Nevertheless, from the success we can only conclude that it must be “almost” an inner-product. The modes are all “seen” and distinguished.
- The “inner-product” is not exactly an inner-product because the set of discrete modes is not complete, i.e. not sufficient to construct *any* possible solution. There is a “continuous” spectrum at the locus of $\omega - ku_0(r) = 0$. From the energy result we can (again) conclude that this part is very small.
- A fine task in functional analysis remains . . .

Epilogue

- The success of NMM is, in a way, too good. At least far better than expected, because the "inner-product" is not a proper inner-product (unless $u_0 = 0$ or uniform) and we can't be sure that it is able to single out each modal contribution.
- Nevertheless, from the success we can only conclude that it must be "almost" an inner-product. The modes are all "seen" and distinguished.
- The "inner-product" is not exactly an inner-product because the set of discrete modes is not complete, i.e. not sufficient to construct *any* possible solution. There is a "continuous" spectrum at the locus of $\omega - ku_0(r) = 0$. From the energy result we can (again) conclude that this part is very small.
- A fine task in functional analysis remains . . .

Epilogue

- The success of NMM is, in a way, too good. At least far better than expected, because the "inner-product" is not a proper inner-product (unless $u_0 = 0$ or uniform) and we can't be sure that it is able to single out each modal contribution.
- Nevertheless, from the success we can only conclude that it must be "almost" an inner-product. The modes are all "seen" and distinguished.
- The "inner-product" is not exactly an inner-product because the set of discrete modes is not complete, i.e. not sufficient to construct *any* possible solution. There is a "continuous" spectrum at the locus of $\omega - ku_0(r) = 0$. From the energy result we can (again) conclude that this part is very small.
- A fine task in functional analysis remains …

Outline

Slowly Varying Duct with Shear Flow

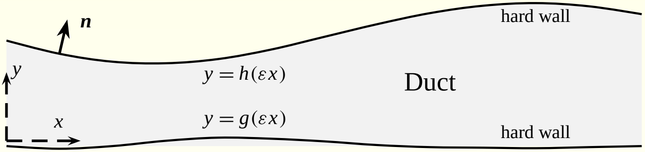

Sketch of geometry: 2-dimensional slowly varying hard-walled duct

Inviscid homentropic mean flow and harmonic perturbations

$$\tilde{\boldsymbol{v}} = \boldsymbol{V} + \mathrm{Re}(\boldsymbol{v}\,\mathrm{e}^{\mathrm{i}\omega t}),$$
$$\tilde{p} = P + \mathrm{Re}(p\,\mathrm{e}^{\mathrm{i}\omega t}),$$
$$\tilde{\rho} = D + \mathrm{Re}(\rho\,\mathrm{e}^{\mathrm{i}\omega t}).$$

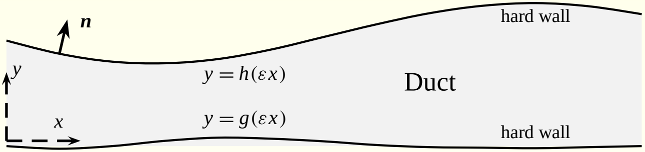

Sketch of geometry: 2-dimensional slowly varying hard-walled duct

Inviscid homentropic mean flow and harmonic perturbations

$$\tilde{\boldsymbol{v}} = \boldsymbol{V} + \mathrm{Re}(\boldsymbol{v}\, \mathrm{e}^{\mathrm{i}\omega t}),$$
$$\tilde{p} = P + \mathrm{Re}(p\, \mathrm{e}^{\mathrm{i}\omega t}),$$
$$\tilde{\rho} = D + \mathrm{Re}(\rho\, \mathrm{e}^{\mathrm{i}\omega t}).$$

Mean Flow and Perturbations

Equations & boundary conditions for the mean flow

$$\boldsymbol{\nabla}\cdot(D\boldsymbol{V}) = 0, \quad D(\boldsymbol{V}\cdot\boldsymbol{\nabla})\boldsymbol{V} = -\boldsymbol{\nabla} P, \quad C^2 = \frac{\gamma P}{D},$$

$$V - g_x U = 0 \text{ at } y = g(\varepsilon x), \quad \text{and} \quad V - h_x U = 0 \text{ at } y = h(\varepsilon x).$$

$$\int_g^h DU \,\mathrm{d}y = \mathcal{F},$$

Equations & boundary conditions for the linearised perturbations

$$\mathrm{i}\omega\rho + \nabla\cdot(\boldsymbol{V}\rho + \boldsymbol{v}D) = 0,$$

$$D\big(\mathrm{i}\omega + \boldsymbol{V}\cdot\nabla\big)\boldsymbol{v} + D\big(\boldsymbol{v}\cdot\nabla\big)\boldsymbol{V} + \rho(\boldsymbol{V}\cdot\nabla)\boldsymbol{V} = -\nabla p,$$

$$p - C^2\rho = 0.$$

$$v - g_x u = 0 \text{ at } y = g(\varepsilon x), \quad \text{and} \quad v - h_x u = 0 \text{ at } y = h(\varepsilon x).$$

Mean Flow and Perturbations

Equations & boundary conditions for the mean flow

$$\nabla\cdot(D\boldsymbol{V})=0,\quad D(\boldsymbol{V}\cdot\nabla)\boldsymbol{V}=-\nabla P,\quad C^2=\frac{\gamma P}{D},$$

$$V-g_xU=0 \text{ at } y=g(\varepsilon x),\quad \text{and}\quad V-h_xU=0 \text{ at } y=h(\varepsilon x).$$

$$\int_g^h DU\,\mathrm{d}y=\mathcal{F},$$

Equations & boundary conditions for the linearised perturbations

$$\mathrm{i}\omega\rho+\nabla\cdot(\boldsymbol{V}\rho+\boldsymbol{v}D)=0,$$

$$D\big(\mathrm{i}\omega+\boldsymbol{V}\cdot\nabla\big)\boldsymbol{v}+D\big(\boldsymbol{v}\cdot\nabla\big)\boldsymbol{V}+\rho(\boldsymbol{V}\cdot\nabla)\boldsymbol{V}=-\nabla p,$$

$$p-C^2\rho=0.$$

$$v-g_xu=0 \text{ at } y=g(\varepsilon x),\quad \text{and}\quad v-h_xu=0 \text{ at } y=h(\varepsilon x).$$

Slowly Varying Mean Flow

- Make dimensionless.
- Introduce slow variable $X = \varepsilon x$.
- For **linear shear flow** of the form

$$U(X, y) = \tau(X) + \sigma(X)(y - g(X)),$$

  an **analytical solution** exists.

Slowly Varying Mean Flow

- Make dimensionless.
- Introduce slow variable $X = \varepsilon x$.
- For **linear shear flow** of the form

$$U(X, y) = \tau(X) + \sigma(X)(y - g(X)),$$

an **analytical solution** exists.

Slowly Varying Mean Flow

- Make dimensionless.
- Introduce slow variable $X = \varepsilon x$.
- For **linear shear flow** of the form

$$U(X, y) = \tau(X) + \sigma(X)(y - g(X)),$$

an **analytical solution** exists.

Slowly Varying Mean Flow (cntd.)

- We have to $\mathcal{O}(\varepsilon^2)$

$$\begin{aligned} (DU)_X + (DV)_y &\simeq 0, \\ D(UU_X + VU_y) + P_X &\simeq 0, \\ P_y &\simeq 0. \end{aligned}$$

- with a parameterised family of solutions

$$\begin{aligned} \sigma &= \lambda D \\ \tau &= \frac{\mathcal{F}}{D(h-g)} - \tfrac{1}{2}\lambda D(h-g). \end{aligned}$$

- The algebraic (Bernoulli-like) equation

$$\frac{1}{2}\tau^2 + \frac{1}{\gamma - 1} D^{\gamma-1} = E,$$

to be solved per X for D, for given flux $\mathcal{F}$, constants λ, E and geometry g, h.

Slowly Varying Mean Flow (cntd.)

- We have to $\mathcal{O}(\varepsilon^2)$

$$\begin{aligned}(DU)_X + (DV)_y &\simeq 0,\\ D(UU_X + VU_y) + P_X &\simeq 0,\\ P_y &\simeq 0.\end{aligned}$$

- with a parameterised family of solutions

$$\begin{aligned}\sigma &= \lambda D\\ \tau &= \frac{\mathcal{F}}{D(h-g)} - \tfrac{1}{2}\lambda D(h-g).\end{aligned}$$

- The algebraic (Bernoulli-like) equation

$$\frac{1}{2}\tau^2 + \frac{1}{\gamma-1}D^{\gamma-1} = E,$$

to be solved per X for D, for given flux $\mathcal{F}$, constants λ, E and geometry g, h.

Slowly Varying Mean Flow (cntd.)

- We have to $\mathcal{O}(\varepsilon^2)$

$$\begin{aligned}(DU)_X + (DV)_y &\simeq 0,\\ D(UU_X + VU_y) + P_X &\simeq 0,\\ P_y &\simeq 0.\end{aligned}$$

- with a parameterised family of solutions

$$\begin{aligned}\sigma &= \lambda D\\ \tau &= \frac{\mathcal{F}}{D(h-g)} - \tfrac{1}{2}\lambda D(h-g).\end{aligned}$$

- The algebraic (Bernoulli-like) equation

$$\frac{1}{2}\tau^2 + \frac{1}{\gamma - 1}D^{\gamma-1} = E,$$

to be solved per X for D, for given flux $\mathcal{F}$, constants λ, E and geometry g, h.

Slowly Varying Modes

To leading order in mean flow we have for the perturbations

$$\begin{aligned}
\mathrm{i}\omega\rho + U\rho_x + D(u_x + v_y) &= -\varepsilon\left[\rho(U_X + V_y) + uD_X + V\rho_y\right],\\
\mathrm{i}\omega u + Uu_x + v\sigma + D^{-1}p_x &= -\varepsilon\left[-D^{-2}D_X p + U_X u + V u_y\right],\\
\mathrm{i}\omega v + Uv_x + D^{-1}p_y &= -\varepsilon\left[V_y v + V v_y\right],\\
p - C^2\rho &= 0.
\end{aligned}$$

Substitute the WKB-Ansatz:

$$[u,\, v,\, p](x, y) = [A,\, B,\, \Phi](X, y; \varepsilon)\, \mathrm{e}^{-\mathrm{i}\int^{x}\kappa(\varepsilon\xi;\varepsilon)\mathrm{d}\xi}$$

with slowly varying mode shapes A, B, Φ and modal wave number κ …

Slowly Varying Modes

To leading order in mean flow we have for the perturbations

$$
\begin{aligned}
\mathrm{i}\omega\rho + U\rho_x + D(u_x + v_y) &= -\varepsilon\left[\rho(U_X + V_y) + uD_X + V\rho_y\right],\\
\mathrm{i}\omega u + Uu_x + v\sigma + D^{-1}p_x &= -\varepsilon\left[-D^{-2}D_X p + U_X u + V u_y\right],\\
\mathrm{i}\omega v + Uv_x + D^{-1}p_y &= -\varepsilon\left[V_y v + V v_y\right],\\
p - C^2\rho &= 0.
\end{aligned}
$$

Substitute the WKB-Ansatz:

$$
[u, v, p](x, y) = [A, B, \Phi](X, y; \varepsilon)\,\mathrm{e}^{-\mathrm{i}\int^x \kappa(\varepsilon\xi;\varepsilon)\mathrm{d}\xi}
$$

with slowly varying mode shapes A, B, Φ and modal wave number κ …

…to obtain to $\mathcal{O}(\varepsilon^2)$

$$\begin{aligned}
\mathrm{i}\Omega\Phi + DC^2(-\mathrm{i}\kappa A + B_y) &= -\varepsilon\left[C^2(UC^{-2}\Phi + DA)_X + (V\Phi)_y\right], \\
\mathrm{i}\Omega A + B\sigma - \mathrm{i}\kappa D^{-1}\Phi &= -\varepsilon\left[(D^{-1}\Phi + UA)_X + VA_y\right], \\
\mathrm{i}\Omega B + D^{-1}\Phi_y &= -\varepsilon\left[UB_X + (VB)_y\right],
\end{aligned}$$

with the Doppler-shifted frequency $\Omega = \omega - \kappa U.$

Pridmore-Brown & Weber Equation

Expand

$$A = A_0 + \varepsilon A_1 + \dots, \;\; B = B_0 + \varepsilon B_1 + \dots, \Phi = \Phi_0 + \varepsilon \Phi_1 + \dots$$

to find to leading order the **Pridmore-Brown equation** in Φ_0.

We write $\Phi_0(X, y) = Q(X)\psi(X, y)$,

$$\Omega^2 \left(\frac{\Phi_{0y}}{\Omega^2} \right)_y + \left(\frac{\Omega^2}{C^2} - \mu^2 \right) \Phi_0 = 0$$

with ψ normalised and Q to be determined below.

*For linear profile $\longrightarrow$ **Weber's Parabolic Cylinder Equation**: standard software.

Expand

$$A = A_0 + \varepsilon A_1 + \ldots,\ \ B = B_0 + \varepsilon B_1 + \ldots, \Phi = \Phi_0 + \varepsilon \Phi_1 + \ldots$$

to find to leading order the **Pridmore-Brown equation** in Φ_0.

We write $\Phi_0(X, y) = Q(X)\psi(X, y)$,

$$\boxed{\Omega^2 \left(\frac{\psi_y}{\Omega^2} \right)_y + \left(\frac{\Omega^2}{C^2} - \mu^2 \right) \psi \ = 0}$$

with ψ normalised and Q to be determined below.

*For linear profile $\longrightarrow$ **Weber's Parabolic Cylinder Equation**: standard software.

Pridmore-Brown & Weber Equation

Expand

$$A = A_0 + \varepsilon A_1 + \ldots, \;\; B = B_0 + \varepsilon B_1 + \ldots, \Phi = \Phi_0 + \varepsilon \Phi_1 + \ldots$$

to find to leading order the **Pridmore-Brown equation*** in Φ_0.

We write $\Phi_0(X, y) = Q(X)\psi(X, y)$,

$$\boxed{\Omega^2 \left(\frac{\psi_y}{\Omega^2}\right)_y + \left(\frac{\Omega^2}{C^2} - \mu^2\right) \psi \;= 0}$$

with ψ normalised and Q to be determined below.

*For linear profile $\longrightarrow$ **Weber's Parabolic Cylinder Equation**: standard software.

Solvability Condition to Determine Amplitude $Q(X)$

By considering a solvability condition for the next order (A_1, B_1, Φ_1) and the usual manipulations we arrive at something like

$$DQ_X = f_1 Q - f_2 Q_X.$$

with solution

$$Q(X) = Q_0 \exp\Big(\int_0^X \frac{f_1(z)}{D(z) + f_2(z)}\,\mathrm{d}z\Big).$$

- For potential mean flow and potential perturbations there exists a *simple adiabatic invariant*, leading to an elegant and simple expression for Q.
- This is probably related to the existence of a *conserved energy*.
- With vortical mean flow there is *no conserved energy*.

Solvability Condition to Determine Amplitude $Q(X)$

By considering a solvability condition for the next order (A_1, B_1, Φ_1) and the usual manipulations we arrive at something like

$$DQ_X = f_1 Q - f_2 Q_X.$$

with solution

$$Q(X) = Q_0 \exp\left(\int_0^X \frac{f_1(z)}{D(z) + f_2(z)}\,\mathrm{dz}\right).$$

- For potential mean flow and potential perturbations there exists a *simple adiabatic invariant*, leading to an elegant and simple expression for Q.
- This is probably related to the existence of a *conserved energy*.
- With vortical mean flow there is *no conserved energy*.

Solvability Condition to Determine Amplitude $Q(X)$

By considering a solvability condition for the next order (A_1, B_1, Φ_1) and the usual manipulations we arrive at something like

$$DQ_X = f_1 Q - f_2 Q_X.$$

with solution

$$Q(X) = Q_0 \exp\left(\int_0^X \frac{f_1(z)}{D(z) + f_2(z)}\,\mathrm{d}z\right).$$

- For potential mean flow and potential perturbations there exists a *simple adiabatic invariant*, leading to an elegant and simple expression for Q.
- This is probably related to the existence of a *conserved energy*.
- With vortical mean flow there is *no conserved energy*.

Solvability Condition to Determine Amplitude $Q(X)$

By considering a solvability condition for the next order (A_1, B_1, Φ_1) and the usual manipulations we arrive at something like

$$DQ_X = f_1 Q - f_2 Q_X.$$

with solution

$$Q(X) = Q_0 \exp\left(\int_0^X \frac{f_1(z)}{D(z) + f_2(z)}\,\mathrm{dz}\right).$$

- For potential mean flow and potential perturbations there exists a *simple adiabatic invariant*, leading to an elegant and simple expression for Q.
- This is probably related to the existence of a *conserved energy*.
- With vortical mean flow there is *no conserved energy*.

Examples

A typical mean flow is described by the problem parameters

$$\lambda = 0.5, \quad D_{\text{in}} = 1, \quad \tau_{\text{in}} = 0.2, \quad \mathcal{F} = 0.4496, \quad E = 2.52, \quad \gamma = 1.4,$$

(i.e. shear $\sigma_{\text{in}} = 0.5$) and the geometry by

$$h(x) = 1 - \tfrac{1}{8}(1 + \tanh(x), \quad g(x) = 0, \quad -3 < x < 3.$$

For the acoustic part we considered

- 4 cut-on right-running modes with $\omega = 13$.
- 1 cut-on left-running mode with $\omega = 2$.
- 1 cut-on left-running mode with $\omega = 4$.

Examples (mean flow)

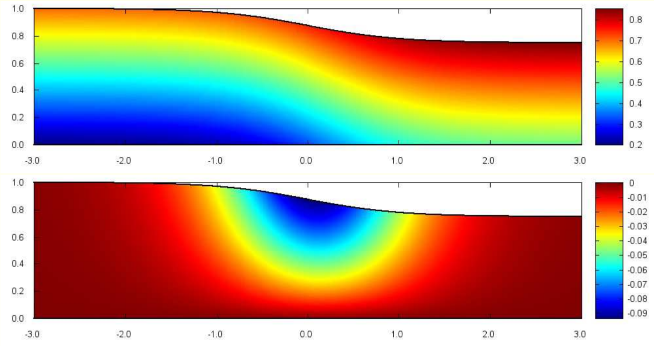

Mean flow U and V in x, y-domain

The flow starts with a shear flow of $U_{\text{in}} = 0.2 + 0.5y$.

Examples (modal axial wave numbers)

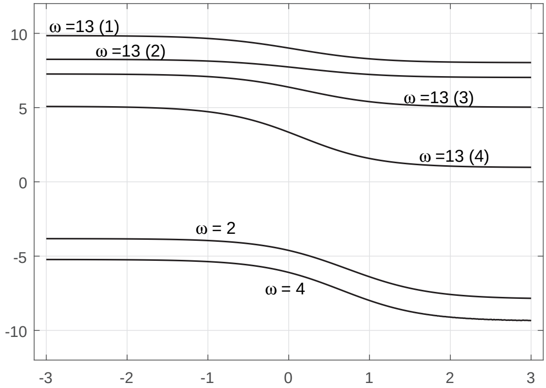

Axial wave numbers κ as function of x.

Question: $\kappa = 0$ is “cut-off”?

Examples (modal axial wave numbers)

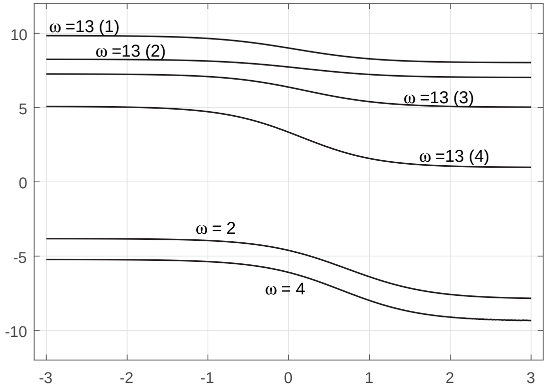

Axial wave numbers κ as function of x.

Question: $\kappa = 0$ is "cut-off"?

Examples (animated snap shots of modes)

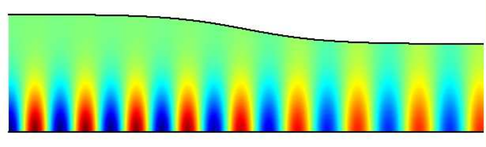

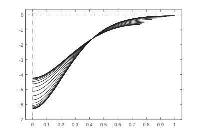

Right-running modal pressure fields for $\omega = 13$ and radial mode number $n = 1, 2, 3, 4$

Examples (animated snap shots of modes)

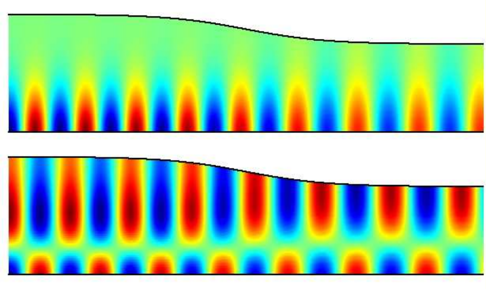

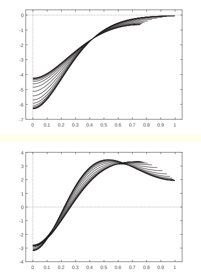

Right-running modal pressure fields for $\omega = 13$ and radial mode number $n = 1, 2, 3, 4$

Examples (animated snap shots of modes)

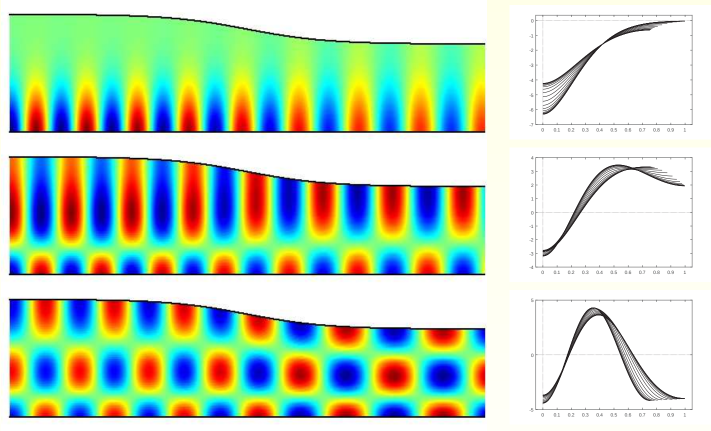

Right-running modal pressure fields for $\omega = 13$ and radial mode number $n = 1, 2, 3, 4$

Examples (animated snap shots of modes)

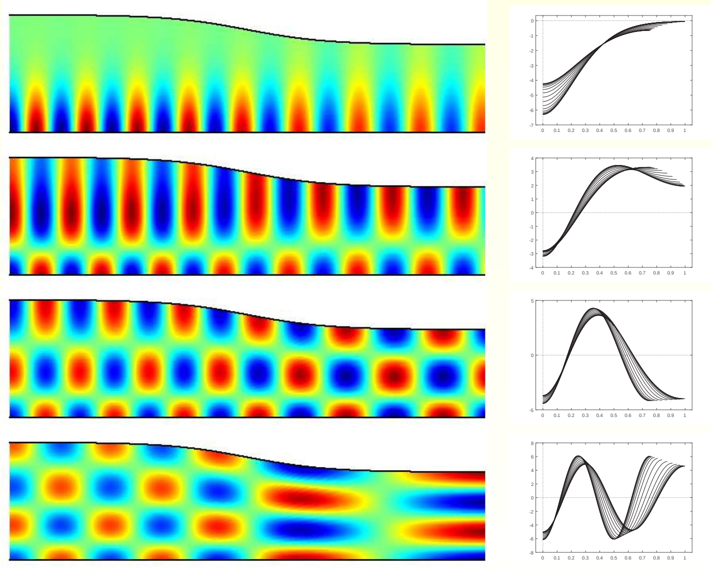

Right-running modal pressure fields for $\omega = 13$ and radial mode number $n = 1, 2, 3, 4$

Examples (animated snap shots of modes)

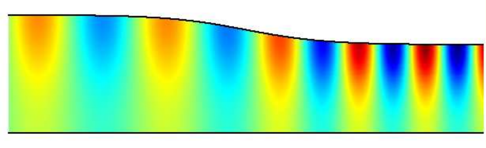

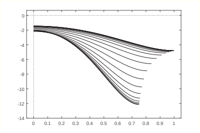

Left-running modal pressure fields for $\omega = 2$ and $\omega = 4$

Examples (animated snap shots of modes)

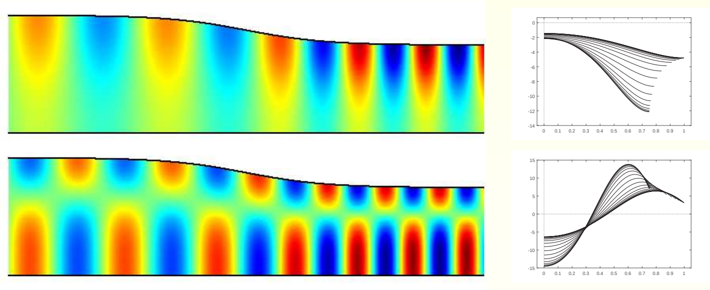

Left-running modal pressure fields for $\omega = 2$ and $\omega = 4$

Interim conclusions

- Slowly varying mean flow of linear shear has analytic solutions.
- A WKB solution of slowly varying modes in linear shear is possible.
- Turning point analysis tbd.
- In contrast to the slowly varying modes in potential mean flow, there is no (simple) adiabatic invariant, and the solution requires some numerical after-care.

Interim conclusions

- Slowly varying mean flow of linear shear has analytic solutions.
- A WKB solution of slowly varying modes in linear shear is possible.
- Turning point analysis tbd.
- In contrast to the slowly varying modes in potential mean flow, there is no (simple) adiabatic invariant, and the solution requires some numerical after-care.

Interim conclusions

- Slowly varying mean flow of linear shear has analytic solutions.
- A WKB solution of slowly varying modes in linear shear is possible.
- Turning point analysis tbd.
- In contrast to the slowly varying modes in potential mean flow, there is no (simple) adiabatic invariant, and the solution requires some numerical after-care.

Interim conclusions

- Slowly varying mean flow of linear shear has analytic solutions.
- A WKB solution of slowly varying modes in linear shear is possible.
- Turning point analysis tbd.
- In contrast to the slowly varying modes in potential mean flow, there is no (simple) adiabatic invariant, and the solution requires some numerical after-care.

Outline

Conclusions

- Interaction of sound with mean flow vorticity.
- Included by the Pridmore-Brown equation for modes in parallel shear flow.
- Instabilities, production of vorticity by mass source.
- Regularisation of ill-posed boundary condition for vanishing boundary layer.
- Integrals of Pridmore-Brown modes produce efficient new mode-matching method
- Slowly varying modes are possible with shear flow, although not with explicit adiabatic invariant.

Conclusions

- Interaction of sound with mean flow vorticity.
- Included by the Pridmore-Brown equation for modes in parallel shear flow.
- Instabilities, production of vorticity by mass source.
- Regularisation of ill-posed boundary condition for vanishing boundary layer.
- Integrals of Pridmore-Brown modes produce efficient new mode-matching method
- Slowly varying modes are possible with shear flow, although not with explicit adiabatic invariant.

Conclusions

- Interaction of sound with mean flow vorticity.
- Included by the Pridmore-Brown equation for modes in parallel shear flow.
- Instabilities, production of vorticity by mass source.
- Regularisation of ill-posed boundary condition for vanishing boundary layer.
- Integrals of Pridmore-Brown modes produce efficient new mode-matching method
- Slowly varying modes are possible with shear flow, although not with explicit adiabatic invariant.

Conclusions

- Interaction of sound with mean flow vorticity.
- Included by the Pridmore-Brown equation for modes in parallel shear flow.
- Instabilities, production of vorticity by mass source.
- Regularisation of ill-posed boundary condition for vanishing boundary layer.
- Integrals of Pridmore-Brown modes produce efficient new mode-matching method
- Slowly varying modes are possible with shear flow, although not with explicit adiabatic invariant.

Conclusions

- Interaction of sound with mean flow vorticity.
- Included by the Pridmore-Brown equation for modes in parallel shear flow.
- Instabilities, production of vorticity by mass source.
- Regularisation of ill-posed boundary condition for vanishing boundary layer.
- Integrals of Pridmore-Brown modes produce efficient new mode-matching method
- Slowly varying modes are possible with shear flow, although not with explicit adiabatic invariant.

Conclusions

- Interaction of sound with mean flow vorticity.
- Included by the Pridmore-Brown equation for modes in parallel shear flow.
- Instabilities, production of vorticity by mass source.
- Regularisation of ill-posed boundary condition for vanishing boundary layer.
- Integrals of Pridmore-Brown modes produce efficient new mode-matching method
- Slowly varying modes are possible with shear flow, although not with explicit adiabatic invariant.

Acknowledgements

I want to acknowledge the contributions of

Ed Brambley,
Mirela Darau,
Werner Lazeroms,
Robert Mattheij,
Martien Oppeneer,
Pieter Sijtsma,
Deepesh Singh,
Johan Slot,
Gregori Vilenski.

and thank them for the stimulating and ever pleasant cooperation.